

Hydroclimate in Africa during the Medieval Climate Anomaly

Sebastian Lüning^{a,*}, Mariusz Gałka^b, Iliya Bauchi Danladi^c, Theophilus Aanuoluwa Adagunodo^d, Fritz Vahrenholt^e

^a Institute for Hydrography, Geoeiology and Climate Sciences, Hauptstraße 47, 6315 Ägeri, Switzerland

^b Department of Biogeography and Palaeoecology, Faculty of Geographical and Geological Sciences, Adam Mickiewicz University, B. Krygowskiego 10, 61-680 Poznań, Poland

^c Department of Geological Engineering, Faculty of Engineering, Mugla Sıtkı Koçman University, 48100 Kotekli-Muğla, Turkey

^d Department of Physics, Covenant University, Ota, Ogun State, Nigeria

^e Department of Chemistry, University of Hamburg, Hamburg, Germany



ARTICLE INFO

Keywords:

Palaeoclimate
Rainfall
North Atlantic Oscillation
Solar forcing
Sahel
East African lakes

ABSTRACT

The Medieval Climate Anomaly (MCA) is a recognized period of distinct pre-industrial climate change, with a core period of 1000–1200 CE. The field of palaeoclimatology has made major progress over the past 15 years during which a great number of high- and medium-resolution case studies were published, reconstructing climate change of the past millennia. In many parts of the world, regional data coverage has now reached a point which allows compiling palaeoclimate maps for well-defined time intervals. Here we present hydroclimatic trend maps for the MCA in Africa based on 99 published study locations. Key hydroclimatic proxy curves are visualized and compared in a series of 16 correlation panels. Proxy types are described and possible issues discussed. Based on the combined MCA dataset, temporal and spatial trends are interpreted and mapped out. Three areas have been identified in Africa in which rainfall seems to have increased during the MCA, namely Tunisia, western Sahel and the majority of southern Africa. At the same time, a reduction in precipitation occurred in the rest of Africa, comprising of NW and NE Africa, West Africa, Eastern Africa and the Winter Rainfall Zone of South Africa. MCA hydroclimate change in Africa appears to have been associated with characteristic phases of ocean cycles, as also supported by modern climate observations. Aridity in Morocco typically coincides with the positive phase of the North Atlantic Oscillation (NAO), whilst increased rainfall in the western Sahel is often coupled to the positive phase of the Atlantic Multidecadal Oscillation (AMO). Reduction in rainfall in the region Gulf of Aden/southern Red Sea to Eastern Africa could be linked to a negative Indian Ocean Dipole (IOD) or a derived long-term equivalent Indian Ocean cycle parameter. The Intertropical Convergence Zone (ITCZ) appears to have been shifted pole-wards during the MCA, for both the January and July positions. MCA hydroclimate mapping revealed major data gaps in the Sahara, South Sudan, Somalia, Central African Republic, Democratic Republic of Congo, Angola, northern Mozambique, Zambia and Zimbabwe. Special efforts are needed to fill these gaps, e.g. through a dedicated structured research program in which new multiproxy datasets are created, based on the learnings from previous African MCA studies.

1. Introduction

Large parts of Africa depend on seasonal rainfall which supplies drinking water and forms the basis for agriculture and food production. Observational precipitation data collected over the past 100 years indicates that African rainfall shows significant variability on year-to-year to decadal time-scales. For example, after rather dry years in the 1980s and 1990s, the Maghreb has now returned to wetter conditions (Nouaceur and Murarescu, 2016). West Africa and the Sahel experienced severe drought during the 1970s and 1980s with a regime shift

towards increased rainfall around 1992 (Badou et al., 2017; Park et al., 2016). Precipitation in South Africa is particularly influenced by multi-year variations without any detectable major regionally aggregated trends in total rainfall (MacKellar et al., 2014). Droughts have been steadily increasing in the Greater Horn of Africa over the past three decades (Rowell et al., 2015), whilst the general development in equatorial eastern Africa is complex, yielding differences in trends for the short and long rainfall seasons (Gitau et al., 2017). In many cases, climate models are unfortunately not yet able to robustly capture the observed trends (e.g. MacKellar et al., 2014; Masih et al., 2014;

* Corresponding author.

E-mail addresses: luening@ifhgk.org (S. Lüning), galka@amu.edu.pl (M. Gałka), fritz.vahrenholt@chemie.uni-hamburg.de (F. Vahrenholt).

Nouaceur and Murarescu, 2016; Rowell et al., 2015). Only recently has it become clear that a significant part of the African rainfall variability is associated with multi-decadal large-scale climate modes of the global oceans (e.g. Masih et al., 2014; Nash et al., 2016; Taye and Willems, 2012; Tierney et al., 2013; Verdon-Kidd and Kiem, 2014). Full integration of such ocean cycles into the models is likely to improve the model skill with regards to multi-decadal regional precipitation trends in Africa.

A second key challenge for hydroclimate simulations is the correct reproduction of centennial-scale trends in African rainfall. African palaeoclimate reconstructions have identified major hydroclimatic trends over the past 2000 years which form important calibration data sets for model hindcast tests (e.g. Chase et al., 2013; Maley and Vernet, 2015; Nash et al., 2016; Stager et al., 2012b; Tierney et al., 2015). Modern African climate variability is a mixture of anthropogenic and natural drivers. A robust understanding of pre-industrial hydroclimate change and possible forcings is needed to be able to distinguish between natural and anthropogenic contributions in modern African rainfall.

Here we are presenting an analysis of centennial-scale hydroclimatic change in Africa for the Medieval Climate Anomaly (MCA), a recognized phase of natural pre-industrial climate change associated with marked temperature and hydroclimatic variability in many parts of the world. The anomaly was first described by Lamb (1965) as ‘Early Medieval Warm Epoch’, which subsequently changed in the literature to ‘Medieval Warm Period’ (MWP). It is generally agreed today that the core period of the MCA comprises ca. 1000–1200 CE, even though different time schemes and durations have historically been used in the literature (e.g. Crowley and Lowery, 2000; Esper and Frank, 2009; Mann et al., 2009). The few existing land temperature reconstructions from Africa with adequate resolution in the last 2000 years suggest a generally warm MCA, but do not allow comprehensive assessment of the continent’s temperature variability during this period (Lüning et al., 2017; Nash et al., 2016; PAGES 2k Consortium, 2013).

In contrast, hydroclimate reconstructions covering the MCA in Africa are more widely available which enabled the PAGES2k Africa group to compile an invaluable hydroclimate synthesis for the past 2000 years based on selected high-resolution datasets (Nash et al., 2016). The group identified several major hydroclimatic trends across the MCA which they reported as general observations in the text, but not in map form. A trend towards increased rainfall is reported for the Sahel, Namibia and the majority of South Africa, whilst drier-than-usual conditions are described for the MCA in the area immediately south of the Sahel, Eastern Africa and the Winter Rainfall Zone of South Africa. No trend information was available for North Africa, Angola, Congo Kinshasa and Madagascar. The group proposed ocean cycles such as Atlantic multi-decadal variability, Indian Ocean Dipole and El Niño–Southern Oscillation (ENSO) as main drivers of the pre-industrial hydroclimatic change in Africa.

Here we are building on the results of Nash et al. (2016) as well as other predecessor papers (e.g. Holmgren and Öberg, 2006; Verschuren, 2004) and aim to take the analysis one step further by mapping the MCA hydroclimate trends in detail across the continent. We are enlarging the dataset by adding case studies that were only recently published and post-date the cut-off date of Nash et al. (2016), or which were excluded by the PAGES2k group due to lower resolution nature, yet may offer useful qualitative insight into the African MCA hydroclimate. Based on the enlarged portfolio of case studies, we add the MCA hydroclimate of North Africa, the eastern Sahel and Madagascar into the African-wide picture and attempt to delineate likely borders of the regions sharing similar trends in MCA hydroclimate. Hydroclimatic change in Africa during the MCA followed characteristic regional patterns whereby knowledge of the distributional trends will ultimately help to better understand the respective driving mechanisms behind the change.

The objective of this paper is to provide a *qualitative* description of regional variability, leaving a fully *quantitative* analysis for later, once

crucial data gaps have been filled. Hydroclimate is intensely linked to climate change. Rain belts are prone to shift and monsoons can intensify or weaken. The analysis of MCA temperature trends in Africa is not part of this study and was documented in a separate contribution (Lüning et al., 2017).

2. Modern hydroclimate elements of Africa

According to the Köppen-Geiger climate classification (e.g. Köppen, 1918), Africa can be grouped into several sub-tropical to tropical climate zones. These include for example the Mediterranean climate of the northern Maghreb, the warm desert climate of the Sahara and Namib deserts, the warm semi-arid climate of the Sahel, the tropical savannah climate of the equator region, the humid subtropical climate of Angola and Zambia, the warm semi-arid climate of Namibia and Zimbabwe, as well as the cold semi-arid and desert climates of South Africa.

African monsoon rains are generally controlled by the seasonal shift of the Intertropical Convergence Zone (ITCZ) where the northeast and southeast trade winds converge, triggering the rise of moisture-laden air which then results in heavy precipitation. The general mechanism brings rain to the Sahel Zone in northern hemisphere summer and to southern Africa in southern hemisphere summer. Nevertheless, the processes are more complex when looked at in detail. In part of the area the rainy season appears to be controlled by migrating mesoscale features associated with jet streams such as the African Easterly Jet and the Turkana Jet (Nash et al., 2016; Nicholson, 2016). In some areas bimodal rainfall occurs, i.e. two rainy seasons. Following the Hadley cell circulation, dry air descends over the arid subtropics, namely the Sahara Desert in the north and the Namib Desert in the south. Case studies suggest that climatic temperature changes influence both the location and width of the ITCZ (Byrne and Schneider, 2016; Sachs et al., 2009; Schneider et al., 2014). Most of South Africa receives summer rain, whilst only the Western Cape area lies in the winter rainfall zone.

Other important hydroclimatic elements are the African Easterly Jet in the western Sahel Zone, the West Africa rainfall dipole, the Congo Air Boundary (CAB), South Atlantic Anticyclone (SAA), South Indian Ocean Anticyclone (SIA) and the South African Winter and Summer Rainfall Zones (WRZ, SRZ). The location and significance for the MCA hydroclimate will be elaborated in detail in the Discussion part of this paper. More detailed descriptions of African modern hydroclimate elements can be found in Nicholson (2000) and Nash et al. (2016).

3. Material and methods

3.1. Literature review

The mapping project is based on an intense iterative literature screening process during which a large number of published African palaeohydroclimate case studies were evaluated towards their temporal coverage, types of climate information and data resolution. Suitable papers including the MCA core period 1000–1200 CE were earmarked for a thorough analysis. A total of 99 African localities with one or more MCA palaeoclimate proxy curves were identified (Fig. 1, Table 1).

3.2. Palaeoclimate archives and data types

MCA climate reconstructions of the high-graded publications comprised of a wide spectrum of natural archives, namely (1) sediment cores from offshore marine, lakes, swamps, peatlands, lagoons and sebkhas, (2) ice cores from ice caps (e.g. Kilimanjaro), (3) cave speleothems, (4) tree rings, (5) fossilized rock hyrax middens, (6) historical river gauge records (e.g. Nilometer), (7) archaeology and (8) age dating of fluvial deposits and geomorphological features. Data types include (a) palaeontology (pollen, diatoms, ostracods, planktonic and benthic foraminifera), (b) inorganic and organic geochemistry (carbon, oxygen, nitrogen and deuterium isotopes; elemental sediment composition; salt

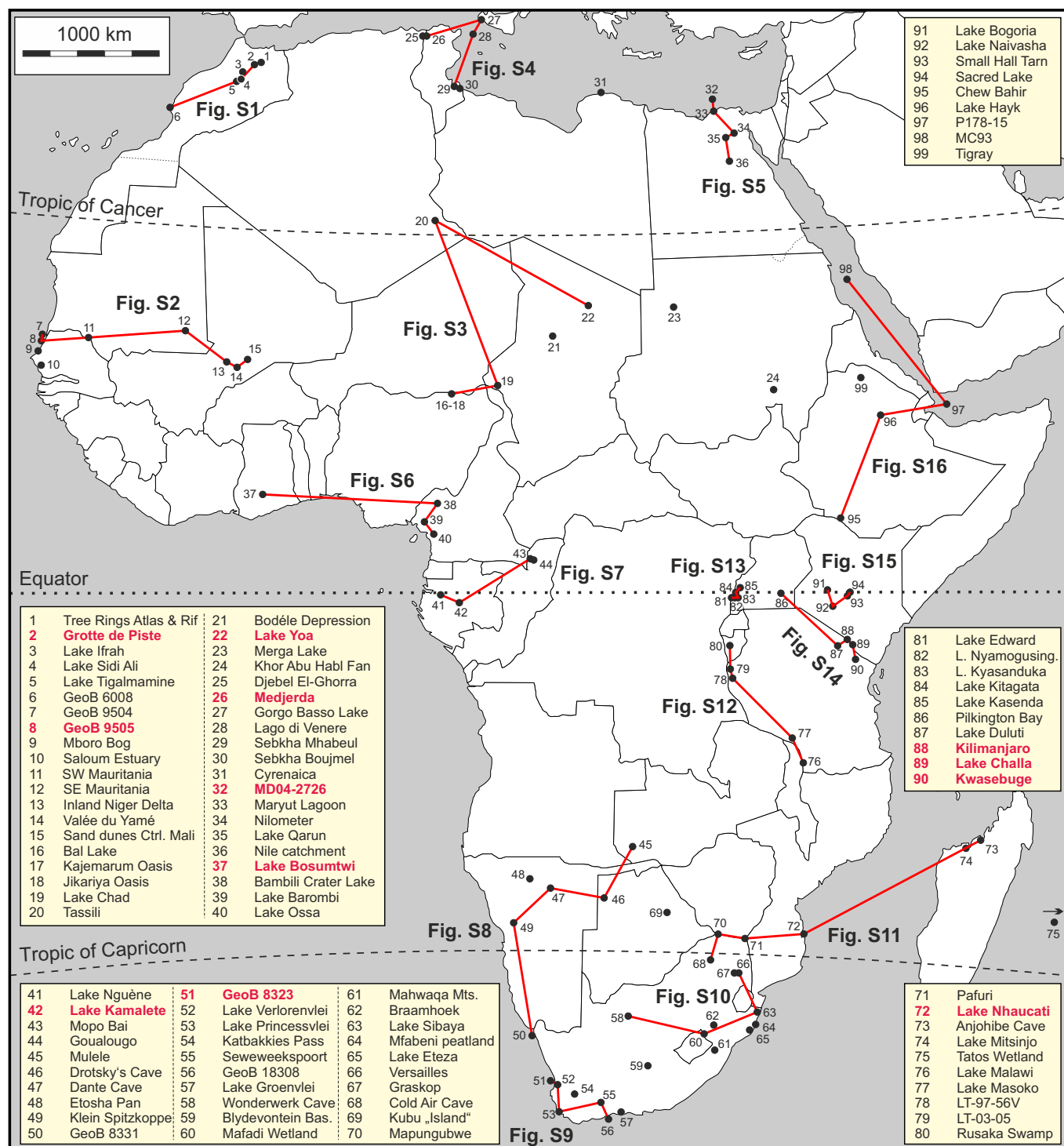


Fig. 1. Location of studied MCA hydroclimate sites (numbered) and correlation panels (red lines, with respective figure number in Data Supplement). Selected sites shown in correlation panels in Figs. 2 and 3 are marked in red in text boxes. (For interpretation of the references to colour in this figure legend, the reader is referred to the web version of this article.)

mineralogy; total organic carbon), (c) geophysics (magnetic susceptibility, optically stimulated luminescence, radio-carbon ^{14}C age dating), (d) sedimentology (facies analysis, sediment petrography, grey levels), and (e) geomorphology.

3.3. Data processing and visualisation

3.3.1. Qualitative

Key information of the identified publications were captured on a

georeferenced online map which is freely available to all interested members of the palaeoclimate science community for research and reference purposes (<http://t1p.de/mwp>). The MCA hydroclimate was visually assessed and compared to the phases preceding and following the anomaly. The MCA conditions were colour-coded with green dots marking a trend towards wetter conditions whilst yellow dots represent drier conditions. The colour-coding provides much-needed initial orientation in the complex global MCA climate puzzle.

Table 1

Hydroclimate study sites of the Medieval Climate Anomaly in Africa. For locations see map in Fig. 1.

Country	Locality	No.	Archive	Proxies	Studies
Morocco	High & Middle Atlas and Rif	1	Trees	Tree rings	Esper et al. (2007), updated by Wassenburg et al. (2013)
Morocco	Grotte de Piste	2	Cave stalagmite	Mg & Sr in stalagmites	Wassenburg et al. (2013)
Morocco	Lake Ifrah	3	Lake core	Grain size, petrography, magnetic susceptibility	Damnat et al. (2016)
Morocco	Lake Sidi Ali	4	Lake core	Diatoms	Lamb et al. (1999)
Morocco	Lake Tigalmamine	5	Lake core	Pollen	Cheddadi et al. (1998)
Morocco	GeoB 6008-1 & 2	6	Marine core	Dust in offshore core	McGregor et al. (2009)
Senegal	GeoB 9504	7	Marine core	Fe/Ca & Al/Ca in offshore core	Nizou et al. (2010, 2011)
Senegal	GeoB 9505	8	Marine core	Fe/Ca in offshore core	Nizou et al. (2010)
Senegal	Mboro bog	9	Peat core	$\delta^{13}\text{C}$, dull quartz	Fall et al. (2010)
Senegal	Saloum Estuary	10	Marine core	Sedimentology	Ausseil-Badie et al. (1991)
Mauritania	SW Mauritania	11	History	History, archaeology	Maley and Vernet (2013)
Mauritania	SE Mauritania	12	History	History, archaeology	Maley and Vernet (2013)
Mali	Inland Niger Delta	13	Fluvial sediments	Fluvial age dating	Maley and Vernet (2015)
Mali	Valée du Yamé	14	History	History, archaeology	Maley and Vernet (2013), Lespez et al. (2011)
Mali	Sand dunes central Mali	15	Aeolian sediments	Aeolian deposits age dating	Stokes et al. (2004)
Nigeria	Bal Lake	16	Lake core	Sr/Ca, ostracods, palynology	Holmes et al. (1999)
Nigeria	Kajemarum Oasis	17	Lake core	Sr/Ca, $\delta^{18}\text{O}$, aeolian dust	Street-Perrott et al. (2000)
Nigeria	Jikariya Oasis	18	Lake core	Aeolian dust	Cockerton et al. (2014)
Chad	Lake Chad	19	Lake and fluvial sediments	Shoreline age dating, sediment profiles, pollen analyses, historical data	Maley and Vernet (2013, 2015)
Algeria	Tassili	20	Trees	Tree rings	Cremaschi et al. (2006)
Chad	Bodé Depression	21	Lake and fluvial sediments	OSL & ^{14}C sediment age dating	Armitage et al. (2015)
Chad	Lake Yoa	22	Lake core	Pollen	Lézine et al. (2011)
Sudan	Merga Lake	23	Lake core	Pollen	Haynes et al. (1979)
Sudan	Khor Abu Habi Fan, White Nile	24	Lake and fluvial sediments	Age-dating of high-energy deposits and shells	Williams et al. (2010)
Algeria	Djebel El-Ghorra	25	Peat core	Pollen	Mustapha and Mohamed (2015)
Tunisia	Medjerda floodplain	26	Fluvial sediments	Fluvial ^{14}C age dating	Zielhofer et al. (2008)
Italy	Gorgo Basso Lake	27	Lake core	Ostracods	Curry et al. (2016)
Italy	Lago di Venere, Pantelleria Island	28	Lake core	Sediment petrography, pollen	Calò et al. (2013)
Tunisia	Sebkha Mhabeul	29	Lake core	Grey scale, sediment petrography	Marquer et al. (2008)
Tunisia	Sebkha Boujemel	30	Lake core	Pollen, sediment petrography	Jaouadi et al. (2016)
Libya	Cyrenaica	31	Cave sediments	Pollen, evaporites	Hunt et al. (2011)
Egypt	MD04-2726	32	Marine core	Si/Al	Revel et al. (2015)
Egypt	Maryut Lagoon	33	Lagoon core	Sedimentology	Flaux et al. (2012)
Egypt	Nilometer	34	Historical measurements	Nile gauge records	Hassan (2007), Kondrashov et al. (2005)
Egypt	Lake Qarun	35	Lake core	Lithology, diatoms, $\delta^{18}\text{O}$, $\delta^{13}\text{C}$ in mollusc shells	Baioumy et al. (2010), Hassan et al. (2012)
Egypt	Nile catchment	36	Fluvial sediments	Fluvial OSL & ^{14}C age dating	Macklin et al. (2015)
Ghana	Lake Bosumtwi	37	Lake core	$\delta^{18}\text{O}$, dust	Shanahan et al. (2009), Mulitza et al. (2010)
Cameroon	Bambili Crater Lake	38	Lake core	Pollen	Izumi and Lézine (2016)
Cameroon	Lake Barombi	39	Lake core	Pollen	Maley and Brenac (1998), Lebamba et al. (2012)
Cameroon	Lake Ossa	40	Lake core	Diatoms	Nguetsop et al. (2004)
Gabon	Lake Nguène	41	Lake core	Pollen	Ngomanda et al. (2007)
Gabon	Lake Kamalete	42	Lake core	Pollen	Ngomanda et al. (2005, 2007)
Rep. Congo	Mopo Bai	43	Swamp core	Dust	Brncic et al. (2009)
Rep. Congo	Goualougo	44	Lake core	Pollen	Brncic et al. (2007)
Zambia	Mulele	45	Peat core	Pollen	Burrough and Willis (2015)
Botswana	Drotsky's Cave	46	Cave stalagmite	Grey level in stalagmite	Railsback et al. (1999), Nash et al. (2006)
Namibia	Dante Cave	47	Cave stalagmite	$\delta^{18}\text{O}$, $\delta^{13}\text{C}$	Sletten et al. (2013)
Namibia	Etosha Pan	48	Lake shore sediments	Shoreline age-dating	Brook et al. (2007)
Namibia	Klein Spitzkoppe	49	Hyrax middens	$\delta^{15}\text{N}$ in hyrax middens	Chase et al. (2009)
South Africa	GeoB 8331	50	Marine core	Pollen, elemental geochemistry	Zhao et al. (2016), Hahn et al. (2016)
South Africa	GeoB 8323	51	Marine core	Elemental geochemistry, grain size	Hahn et al. (2016), Granger et al. (2017)
South Africa	Lake Verlorenvlei	52	Lake core	Diatoms	Stager et al. (2012a)
South Africa	Lake Princessvlei	53	Lake core	Diatoms	Kirsten and Meadows (2016)
South Africa	Katbakkies Pass	54	Hyrax middens	$\delta^{13}\text{C}$ & $\delta^{15}\text{N}$ in hyrax middens	Chase et al. (2015)
South Africa	Seweweekspoort	55	Hyrax middens	$\delta^{13}\text{C}$ & $\delta^{15}\text{N}$ in hyrax middens	Chase et al. (2013)
South Africa	GeoB18308	56	Marine core	Elemental & organic geochemistry, ostracods, foraminifera	Hahn et al. (2017)
South Africa	Lake Groenvlei	57	Lake core	Geochemistry, mineralogy, isotopic & granulometric analyses	Wündsch et al. (2016)
South Africa	Wonderwerk Cave	58	Cave stalagmite	$\delta^{13}\text{C}$, $\delta^{18}\text{O}$, grey colour & luminescence in stalagmite	Brook et al. (2015)
South Africa	Blydefontein basin	59	Lake and fluvial sediments, hyrax middens	Pollen	Scott et al. (2005)
Lesotho	Mafadi Wetland	60	Wetland core	Sedimentary petrography, pollen, diatoms	Fitchett et al. (2017)
South Africa	Mahwaqa Mountain	61	Wetland core	Pollen	Neumann et al. (2014)
South Africa	Braamhoek Wetland	62	Wetland core	Pollen, $\delta^{13}\text{C}$, $\delta^{15}\text{N}$	Norström et al. (2014, 2009)

(continued on next page)

Table 1 (continued)

Country	Locality	No.	Archive	Proxies	Studies
South Africa	Lake Sibaya	63	Lake core	Diatoms, pollen $\delta^{13}\text{C}$, $\delta^{15}\text{N}$	Stager et al. (2013), Neumann et al. (2008)
South Africa	Mfabeni peatland	64	Peatland core	Pollen	Baker et al. (2014)
South Africa	Lake Eteza	65	Lake core	Pollen	Neumann et al. (2010)
South Africa	Versailles	66	Wetland core	Pollen	Breman et al. (2012)
South Africa	Graskop	67	Wetland core	Pollen	Breman et al. (2012)
South Africa	Cold Air Cave	68	Cave stalagmite	Grey scale of stalagmite	Stager et al. (2013)
Botswana	Kubu "Island"	69	Trees	Baobab tree age dating	Riedel et al. (2012)
South Africa	Mapungubwe National Park	70	Trees	$\delta^{13}\text{C}$	Woodborne et al. (2016), Huffman and Woodborne (2016), Huffman (1996)
South Africa	Pafuri	71	Trees	$\delta^{13}\text{C}$	Woodborne et al. (2015)
Mozambique	Lake Nhuacati	72	Lake core	Diatoms	Ekblom and Stabell (2008)
Madagascar	Anjohibe Cave	73	Cave stalagmite	$\delta^{18}\text{O}$, $\delta^{13}\text{C}$	Burns et al. (2016), Voarintsoa et al. (2017), Scroxton et al. (2017)
Madagascar	Lake Mitsinjo	74	Lake core	Pollen	Matsumoto and Burney (1994)
Mauritius	Tatots Wetland	75	Wetlands core	Pollen, diatoms, $\delta^{18}\text{O}$, $\delta^{13}\text{C}$, sediment petrography	de Boer et al. (2014)
Malawi	Lake Malawi	76	Lake core	Diatoms	Johnson et al. (2004)
Tanzania	Lake Masoko	77	Lake core	Diatoms, pollen, charcoal	Barker et al. (2000), Vincens et al. (2003), Thevenon et al. (2003)
Tanzania	Lake Tanganyika (LT-97-56V)	78	Lake core	Ostracods	Alin and Cohen (2003)
Tanzania	Lake Tanganyika (LT03-05)	79	Lake core	Diatoms	Stager et al. (2009)
Burundi	Rusaka Swamp	80	Swamp core	Pollen	Izumi and Lézine (2016)
Uganda	Lake Edward	81	Lake core	$\delta^{18}\text{O}$, $\delta^{13}\text{C}$, Mg	Russell and Johnson (2005, 2007)
Uganda	Lake Nyamogusingiri	82	Lake core	Diatoms	Mills et al. (2014)
Uganda	Lake Kyasanduka	83	Lake core	Diatoms	Mills et al. (2014)
Uganda	Lake Kitagata	84	Lake core	Magnetic susceptibility, mineralogy, TOC	Russell et al. (2007)
Uganda	Lake Kasenda	85	Lake core	$\delta^{18}\text{O}$, $\delta^{13}\text{C}$, diatoms	Ryves et al. (2011), Ssemmanda et al. (2005)
Uganda	Pilkington Bay, Lake Victoria	86	Lake core	Diatoms	Stager et al. (2005, 2003)
Tanzania	Lake Duluti	87	Lake core	Pollen, diatoms	Öberg et al. (2013)
Tanzania	Kilimanjaro	88	Ice core	$\delta^{18}\text{O}$ in ice core	Thompson et al. (2002)
Tanzania	Lake Challa	89	Lake core	BIT Index	Buckles et al. (2016)
Tanzania	Kwasebuge peat bog	90	Peat core	Pollen	Finch et al. (2016)
Kenya	Lake Bogoria	91	Lake core	$\delta^{18}\text{O}$, $\delta^{13}\text{C}$, salt mineralogy	De Cort et al. (2013)
Kenya	Lake Naivasha	92	Lake core	Pollen, diatoms, petrography	Lamb et al. (2003), Verschuren et al. (2000), Verschuren (2001)
Kenya	Small Hall Tarn Lake, Mt. Kenya	93	Lake core	$\delta^{18}\text{O}$ of diatoms	Barker et al. (2001)
Kenya	Sacred Lake	94	Lake core	$\delta^{18}\text{O}$, $\delta^{13}\text{C}$, δD	Konecky et al. (2014)
Ethiopia	Chew Bahir basin	95	Lake core	K as dust proxy	Foerster et al. (2015)
Ethiopia	Lake Hayk	96	Lake core	$\delta^{18}\text{O}$, $\delta^{13}\text{C}$, pollen, diatoms	Lamb et al. (2007), Ghinassi et al. (2012)
Yemen	P178-15	97	Marine core	δD	Tierney et al. (2015)
Sudan	MC93, Red Sea	98	Marine core	Planktic foraminifera	Edelman-Furstenberg et al. (2009)
Ethiopia	Highlands of Tigray	99	Lake core	^{14}C dating of organic-rich layers	Dramis et al. (2003)

3.3.2. Quantitative

In order to robustly document, visualise and analyse MCA hydroclimatic variability, all relevant climate curve data was collected in digital form for flexible plotting and curve correlation. The tabulated data was retrieved (a) from palaeoclimate online data repositories (mainly Pangaea, NOAA's National Climatic Data Center NCDC and data supplements of papers), (b) from authors by email request and (c) by digitizing and vectorising using WebPlotDigitizer (<https://automeris.io/WebPlotDigitizer/>). Data sources for each site are listed in Tables S1–S4.

All curve data have been loaded into Lloyd's Register's software IC™ which serves as a common database and correlation tool in the MCA mapping project. IC™ was originally developed for geological well correlations in the areas of water, minerals and petroleum exploration. The software reliably handles large amounts of fully customizable curve data types related to georeferenced wells. By way of technology transfer we are introducing well correlation software to the field of the climate sciences which allows fast and flexible comparison of climate curves. Another advantage is the advanced visualisation and shading of peak and trough curve anomalies, a functionality which lacks in most standard spreadsheet software packages. See Lüning et al. (2017) for details on the workflow.

3.4. Challenges

Like any other regional palaeoclimatic synthesis, the current Africa hydroclimatic MCA mapping effort is subjected to a number of challenges. Palaeoclimatology is not an exact mathematical science, nevertheless provides crucial data for the palaeoclimatological context and model calibration. A probabilistic approach is needed whereby the most likely scenario is selected from the set of available proxies. Issues identified in the current synthesis include (1) low resolution palaeoclimatic data, (2) limited age control, (3) validity of palaeoclimate interpretation, (4) conflicting information from multiple proxies, (5) seasonal vs. annual significance. See Lüning et al. (2017) for a more detailed discussion.

4. MCA hydroclimate study sites in Africa

A total of 99 study sites have been identified in Africa that inform about MCA hydroclimate. The greatest density of sites is found in Morocco, Tunisia, Egypt, western Sahel, southern Africa and East Africa (Fig. 1, Table 1). Detailed site descriptions and hydroclimate correlation panels can be found in the Supporting Information to this paper (texts and Tables S1–S4, Figs. S1–S16). Two correlation panels with 12 characteristic sites from the study area are illustrated in Figs. 2 and 3 to facilitate the discussion.

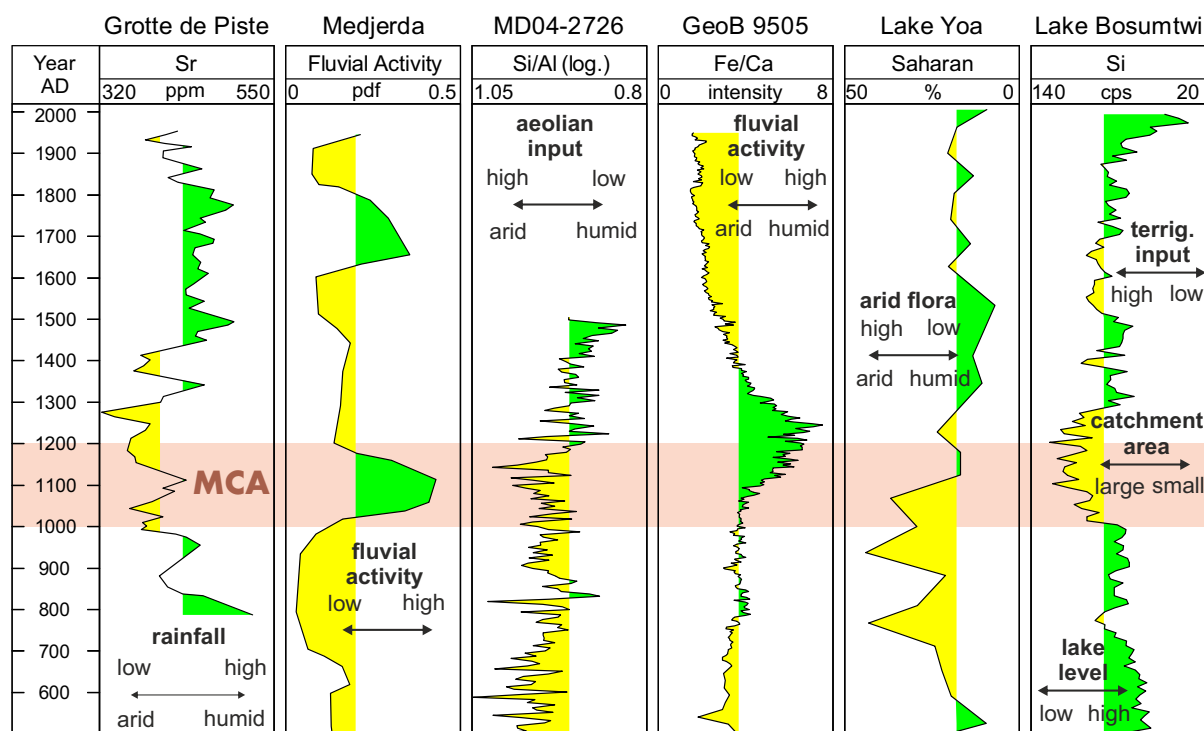


Fig. 2. Hydroclimate development of northern and West Africa during the past 1500 years based on palaeoclimate proxies of selected sites. Grotte de Piste, Morocco (Wassenburg et al., 2013); Medjerda Floodplain, Tunisia (Zielhofer et al., 2008); piston core MD04-2726, Egypt (Revel et al., 2015); offshore core GeoB 9505, Senegal (Nizou et al., 2010); Lake Yoa, Chad (Lézine et al., 2011); Lake Bosumtwi, Ghana (Shanahan et al., 2009). Site names highlighted in red in text boxes of location map in Fig. 1. (For interpretation of the references to colour in this figure legend, the reader is referred to the web version of this article.)

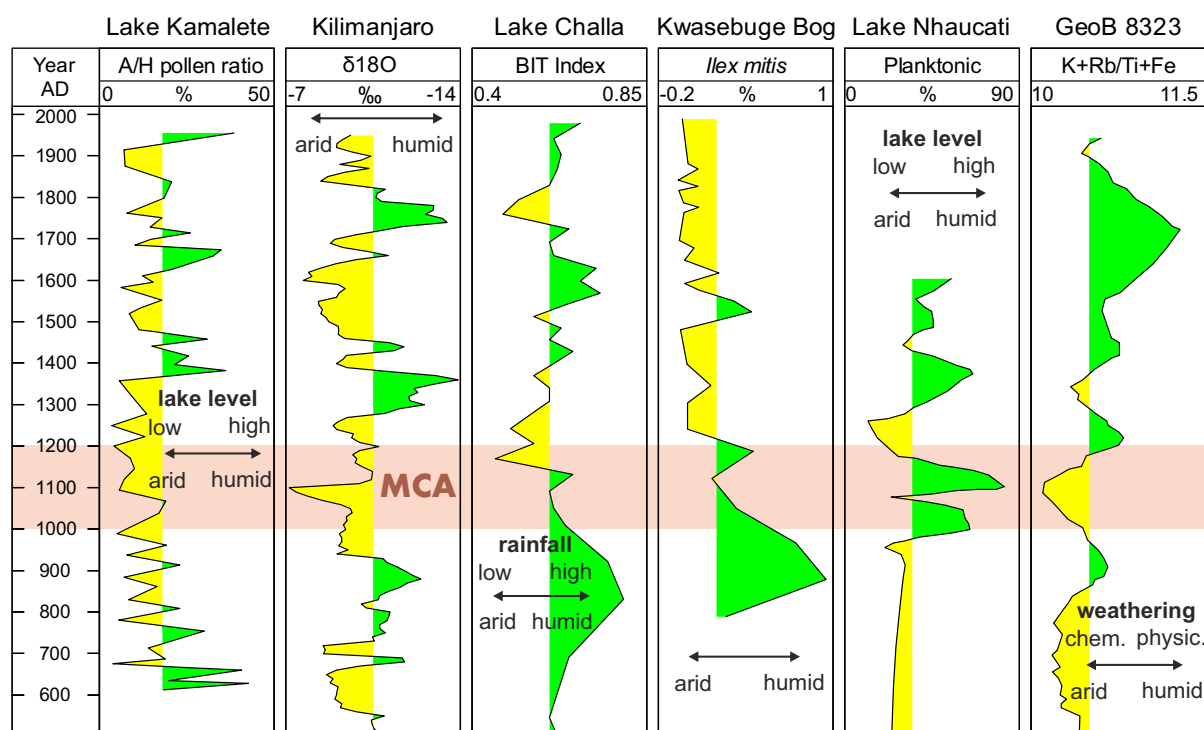


Fig. 3. Hydroclimate development of West, East and southern Africa during the past 1500 years based on palaeoclimate proxies of selected sites. Lake Kamalete, Gabon (Ngomanda et al., 2007); Kilimanjaro NIF2 ice core, Tanzania (Thompson et al., 2002); Lake Challa, Tanzania (Buckles et al., 2016); Kwasebuge Bog, Tanzania (Finch et al., 2016); Lake Nhaucati, Mozambique (Ekblom and Stabell, 2008); GeoB 8323, South Africa (Hahn et al., 2016). Site names highlighted in red in text boxes of location map in Fig. 1. (For interpretation of the references to colour in this figure legend, the reader is referred to the web version of this article.)

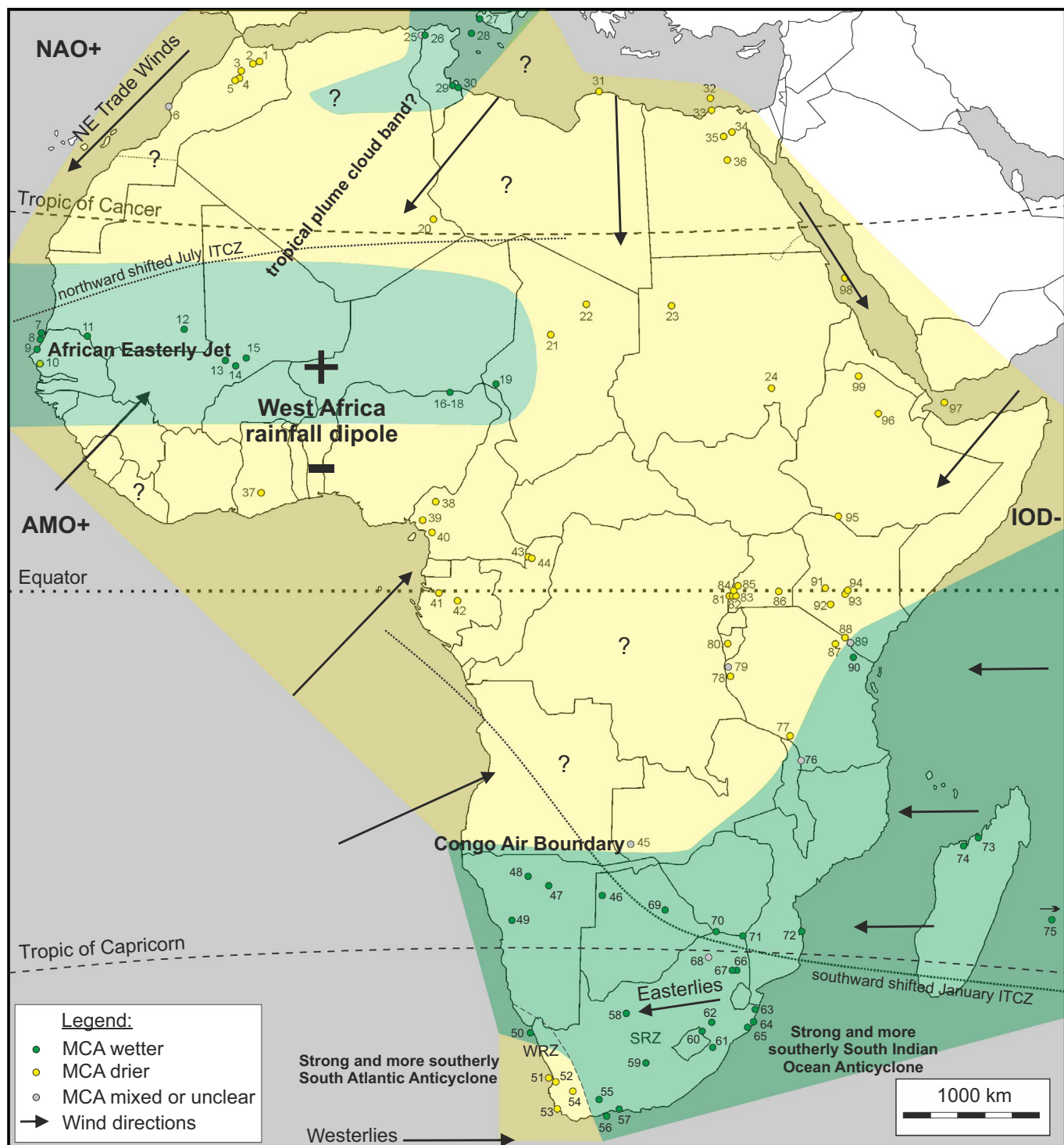


Fig. 4. Hydroclimatic trends during the MCA showing regions with change to drier (yellow) and wetter (green) conditions. Colour-coded circles refer to study sites, numbers as used in table and text. Also shown are hydroclimatic elements relevant to MCA hydroclimatic change, as discussed in the text. Arrows represent major wind directions. (For interpretation of the references to colour in this figure legend, the reader is referred to the web version of this article.)

5. Discussion

The African MCA hydroclimate patterns extracted from the case studies have been mapped out on a continental scale (Fig. 4). Whilst in some areas rainfall increased during the MCA, a reduction in precipitation occurred in others. Possible climatic drivers are discussed, also taking into account hydroclimatic relationships observed from modern times.

5.1. North Africa

The MCA in North Africa was generally characterized by a drying trend that is well documented in Morocco and Egypt (Figs. 2, 4, S1, S5). An exception is Tunisia where MCA hydroclimate appears to have been more humid (Fig. 2, S4). The wet corridor extended northeastward into Sicily. The southwestern termination of the MCA wet zone is unclear due to lack of studies from Algeria. Very similar hydroclimatic trends have been observed in North Africa over the past 100 years, with

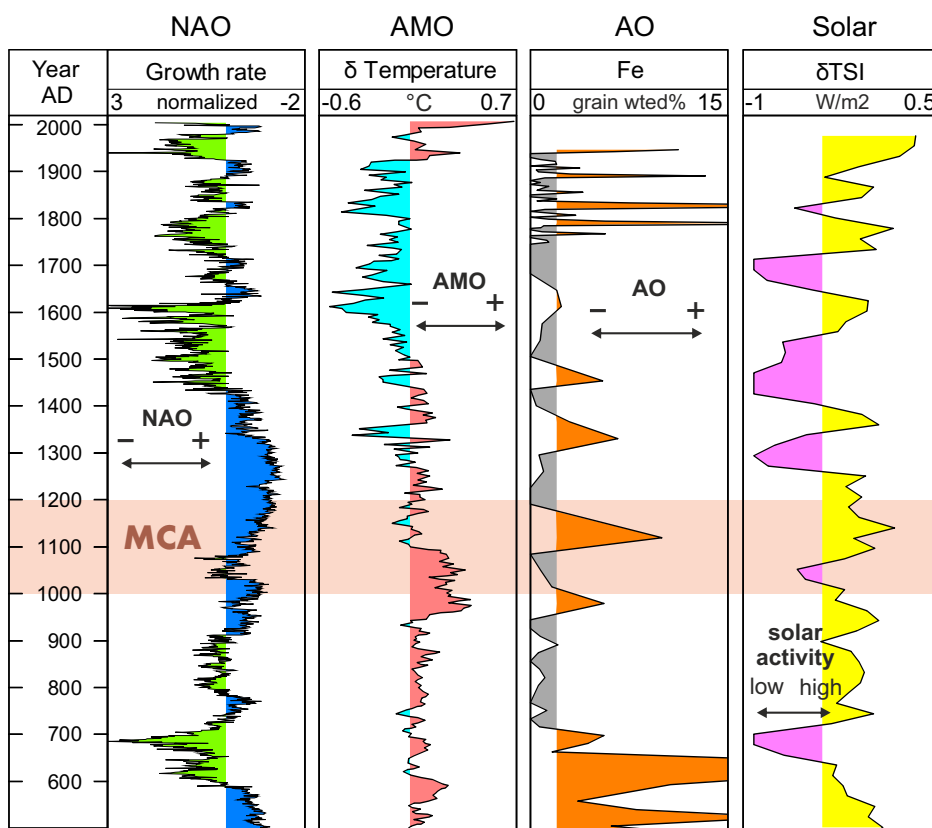


Fig. 5. Overview of potential MCA climate drivers. North Atlantic Oscillation - NAO, stalagmite growth rate (Baker et al., 2015); Atlantic Multidecadal Oscillation - AMO, temperature anomaly (Mann et al., 2009); Arctic Oscillation - AO, Fe grains weighted percentage (Darby et al., 2012); Solar Activity, changes in total solar irradiance - TSI (Steinhilber et al., 2012).

increased precipitation in Tunisia and reduced amounts of rain in the rest of North Africa during the cold season (Hoerling et al., 2012).

Drier conditions in NW Africa and southern Iberia are typically associated with a positive phase of the North Atlantic Oscillation (NAO) that comes with a strong high pressure system off NW Africa (Lamb and Peppler, 1987). This relationship holds also true for the MCA which was dominated by NAO+ conditions as documented by palaeoclimatic reconstructions (Fig. 5). The NAO turned positive around 1000 CE (or even earlier) and generally stayed in the NAO+ state until about 1430 CE (Baker et al., 2015; Olsen et al., 2012; Trouet et al., 2009; Wassenburg et al., 2013). During NAO+ phases, Central Europe and Scandinavia typically experience a more humid climate, something which again was confirmed to be the case during the MCA (Trouet et al., 2009). The NAO has been mostly in its positive phase during the 20th and early 21st centuries, except for two decades of the 1950s and 60s. This may explain the similarity of hydroclimate patterns of the MCA and the last 100 years.

Also the Arctic Oscillation (AO) may play a role here. A positive AO is typically associated with dry conditions in Morocco and the Mediterranean (Givati and Rosenfeld, 2013). According to a reconstruction by Darby et al. (2012), the AO appears to have been moderately elevated 950–1200 CE (Fig. 5), which matches well with the documented reduction in MCA rainfall in Morocco and Egypt (Fig. 4).

5.2. Sahel zone

Hydroclimate during the MCA became more humid in the western and central Sahel, whereas more arid conditions existed in the eastern Sahel (Figs. 2, 4, S2, S3). The border between the two zones appears to have been in the middle of the continent in western Chad, east of Lake Chad. Whilst the earliest part of the MCA in the western Sahel was still rather dry or transitional, generally wetter conditions occurred after 1050 CE and lasted for the majority of the MCA (Fig. S2). The humid

phase ended sometime between 1300 CE and 1400 CE.

Due to the lack of data from Algeria, it is unclear if the western Sahel MCA wet belt was linked to the humid zone in Tunisia (Fig. 4). The two areas might have been connected by diagonal elongated cloud bands, so called tropical plumes, which occasionally couple the subtropical and tropical areas as a result of upper-level disturbances (Fröhlich and Knippertz, 2008; Maley, 2010; Maley and Vernet, 2015; Skinner and Poulsen, 2016). Modern satellite data have documented the southwestward intrusion of upper-level troughs from the central Mediterranean through the Algerian Sahara into the western Sahel zone (Fröhlich et al., 2013; Knippertz and Fink, 2008, 2009; Knippertz and Martin, 2005). Tropical plumes and troughs may therefore have fed the increase in MCA humidity in the western Sahel, sourcing moisture from both the Mediterranean and tropical Atlantic. Increased precipitation might have also occurred over the Saharan part of the trough in Algeria, but it cannot be excluded that clouds simply bypassed this zone without raining out (pers. comm. Peter Knippertz, June 2017).

The increase in MCA western Sahel precipitation may also be related to the generally positive phase of the Atlantic Multidecadal Oscillation (AMO) at this time (Kuhnert and Miltz, 2011; Mann et al., 2009) (Fig. 5) which typically increases moisture flux into the western Sahel from Atlantic sources in the south and west (Delworth et al., 2007; Martin and Thorncroft, 2014; Zhang and Delworth, 2006). According to Ting et al. (2011) the predominant precipitation pattern associated with the positive phase of the AMO is a northward shifted Atlantic ITCZ, resulting in increased rainfall from the western Sahel across the tropical North Atlantic to Central America.

5.3. West and Central Africa

West and Central Africa south of the Sahel zones appears to have been drier during the MCA (Figs. 2–4). The palaeohydroclimate map is mostly based on a cluster of studies in Cameroon, Gabon and Congo-Brazzaville (Figs. S6, S7). Unfortunately, there are hardly any data from

the coastal countries north of the Gulf of Guinea. The only exception is Lake Bosumtwi in Ghana (Site 37) which provides rare and valuable insight into MCA hydroclimate in this region (Figs. 2, S6). Data from the large area of Congo-Kinshasa and Angola are absent.

Monsoonal rainfall in West and Central Africa is controlled by seasonal shifts of the Intertropical Convergence Zone (ITCZ), jet streams, sea surface temperatures in the Gulf of Guinea, and the great seasonal temperature and humidity differences between the Sahara and the equatorial Atlantic Ocean. The rain-bearing summer winds load moisture over the Atlantic which is then carried landward where it is released as rain.

The MCA pattern with humidification in the western Sahel and drying in the Gulf of Guinea coastal belt represents one of four major modes of rainfall variability over West Africa, termed the “West Africa rainfall dipole” which has its node at roughly 10°N (Losada et al., 2012; Maley, 2010; Maley and Vernet, 2015; Nicholson, 2013) (Fig. 4). Other possible dipole modes comprise an inverted trend (Sahel dry/Guinea wet), both zones wet and both zones dry. The Sahel wet/Guinea dry mode observed during the MCA is typically associated with a northward displacement of the African Easterly Jet (Nicholson, 2013). The pattern is also known from most recent times. Dong and Sutton (2015) mapped changes in precipitation in West Africa comparing the periods 1964–1993 and 1996–2011 and documented a typical Sahel wet/Guinea dry dipole. Odoulami and Akinsanola (2017) documented a similar dipole pattern for the trends 1998–2013.

5.4. Eastern Africa

The vast majority of Eastern Africa during the MCA was dominated by dry conditions (Figs. 3, 4, S12–S16). The dry MCA zone appears to be connected to similar drying trends in West and Northeast Africa. Several study sites at the southern end of Eastern Africa have a transitional character with increased signs of humidity during the MCA. Lake Challa on the lower east slope of Mount Kilimanjaro in the border area of Tanzania and Kenya (Site 89) is characterized by a wet phase that commences at 700 CE and reaches well into the MCA until 1150 CE when climate turned arid (Fig. 3). About 110 km to the south in the Kwasebuge peat bog (site 90) the wet phase appears even more pronounced during the MCA (Fig. 3). The MCA trend in northern Madagascar is already fully humid (Fig. S11).

The MCA hydroclimatic border between drier Eastern Africa and more humid southern Africa is interpreted to run southwestward, based on a MCA transition character in Lake Malawi (site 76) in case the BSI represents a hydroclimate proxy here (Fig. S12). Another hydroclimatic border point is interpreted for the wetland site of Mulele in SW Zambia (Fig. S8). Here, the generally dry MCA is immediately preceded by an intense wet spike that partly reached into the early MCA and may indicate proximity to the wet MCA region. More data are clearly needed to reliably map out in detail the wet/dry MCA distribution in this transition zone.

On a larger-scale perspective, the southern African wet MCA zone may be connected to the southernmost tip and east coast of India where precipitation increased during the MCA as well (e.g. Chauhan et al., 2010; Sandeep et al., 2015; Zorzi et al., 2015). The western part of India, however, was characterized by a drier MCA (e.g. Prasad et al., 2014; Shankar et al., 2006; Thamban et al., 2007), possibly linked across the Indian Ocean to the corresponding dry zone in Eastern Africa.

Rainfall in Eastern Africa occurs in two wet seasons - in March to May and in October to December. Notably, the dry MCA area of Eastern Africa has also become drier in modern times over the past 70 years (Hua et al., 2016; Ongoma and Chen, 2017). Hydroclimate in Eastern Africa is influenced by the Indian Ocean Dipole (IOD), an oscillation of sea-surface temperatures in this ocean. The negative phase of the IOD typically leads to drought conditions in a coastal belt that stretches from Eastern Africa to the southern Arabian Peninsula until western

India. During the positive IOD phase, hydroclimate in this zone changes to more humid conditions with heavy rains (Saji et al., 1999). It could be speculated that reduced rainfall in Eastern Africa during the MCA might have been related to an extended period of a predominantly negative IOD, i.e. a respective long term shift in the Indian Ocean SST gradient. Unfortunately, IOD reconstructions reaching back one millennium or more do not yet exist (pers. comm. Nerilie Abram, June 2017). A hydroclimatological synthesis for Eastern Africa by Tierney et al. (2013) for the past 700 years provides evidence for systematic long-term changes and Indian Ocean involvement. Regional dry/wet patterns reversed from the MCA to the Little Ice Age indicating a climatic switch in the Indian Ocean.

5.5. Southern Africa

Southern Africa became wetter during the MCA, except for the Winter Rainfall Zone (WRZ) in western South Africa (Figs. 3, 4, S8–S11). Summer rain sourced from the Easterlies appears to have intensified, whereas the winter rain that originates in the Atlantic to the west was reduced (Hahn et al., 2016; Hahn et al., 2017). Precipitation in the Summer Rainfall Zone (SRZ) increased because the South Indian Ocean Anticyclone (SIA) strengthened and shifted (together with the ITCZ) to a more southerly position, which intensified the rain-bearing tropical Easterlies. On the Atlantic side, the South Atlantic anticyclone (SAA) strengthened and shifted to a more southerly position as well which pushed the rain-bearing Westerlies so far south and away from land that they no longer intercepted the continent (Cohen and Tyson, 1995; Hahn et al., 2016; Hahn et al., 2017; Stager et al., 2012a; Woodborne et al., 2016; Woodborne et al., 2015; Zhao et al., 2016). Opposite hydroclimatic trends for the WRZ and SRZ have been observed during most of the Holocene (Zhao et al., 2016).

The interpreted border between a wet MCA to the south (Namibia) and dry MCA to the north (Angola) is marked by the Congo Air Boundary (CAB). Towards eastern Africa, the border assumes a northeast trend (Fig. 4) which in part corresponds to the course of the CAB. The CAB has already previously been identified by Tierney et al. (2011) as a fundamental controlling mechanism for hydroclimate in the African tropics, separating moisture transport from the Indian Ocean and Atlantic Ocean.

The anti-phase hydroclimatic relationship between the southern African SRZ and Eastern Africa is a well-established pattern on inter-annual to millennial time scales (Ekblom and Stabell, 2008; Norström et al., 2014; Zhang et al., 2015). This rainfall dipole is tentatively coupled with the Indian Ocean Dipole (IOD) and El Niño-Southern Oscillation (ENSO). During a “wet in the south and dry in the north” dipole, such as during the MCA, there are warm sea surface temperatures (SSTs) over the central Indian Ocean and cold SSTs over the western Indian Ocean (Zhang et al., 2015).

5.6. African MCA hydroclimate trends

Our study has successfully confirmed the majority of hydroclimatic MCA trends described by Nash et al. (2016), i.e. increased rainfall in the western Sahel, Namibia and the majority of South Africa, with drier-than-usual conditions in the area immediately south of the Sahel, Eastern Africa and the Winter Rainfall Zone of South Africa. Based on our palaeoclimate mapping, the observation of transitional hydroclimatic signatures at certain sites and integration of modern climate boundary elements, we attempt to delineate borders for the different hydroclimatic MCA trend sectors (Fig. 4). Ongoing and future studies by the palaeoclimate community are needed to verify and modify this provisional first MCA hydroclimate map of Africa.

In deviation to Nash et al. (2016) we interpret that the eastern Sahel was drier than usual during the MCA (Fig. 4). We are adding North Africa to the picture and interpret a dry trend for this region, too. The only exception appears to be Tunisia/Sicily where rainfall has increased

during the MCA. The wet eastern Maghreb may or may not be connected across the Sahara to the humidification observed in the western Sahel (Fig. 4). Finally, we are seeing evidence for an MCA wet trend along the East African coast that reaches from South Africa as far north as Kenya. New data from Madagascar and transitional hydroclimate signatures in Tanzania support this interpretation (Figs. 3, S11, S14). New studies in coastal Mozambique, Tanzania and Kenya are necessary to follow up on this concept.

A recent synthesis of Northern Hemisphere hydroclimate variability during the past 1200 years by Ljungqvist et al. (2016) is based on 196 published study locations and also includes 8 proxy records from Africa north of the equator. These are Grotte de Piste (Site 2), Lake Nguène (Site 41), Lake Kamaléti (Site 42), Lake Bosumtwi (Site 37), Lake Edward (Site 81), Lake Naivasha & Crescent Island Crater (Site 92), Lake Chala (Site 89). The authors document characteristic patterns of alternating moisture regimes across the Northern Hemisphere which show a high degree of continuity until today. Owing to the low number of sites from Africa, their hydroclimate interpretations naturally remain somewhat patchy for this region. However, the West African MCA drying trend along the Gulf of Guinea coast is readily identified by Ljungqvist et al. (2016) in their anomaly maps of the years 1000s to 1200s AD. In contrast, the wet MCA anomaly proposed by Ljungqvist et al. (2016) for Morocco - based on the single site of Grotte de Piste - is more ambiguous, as it differs from our findings. Notably, all chosen African sites for the Northern Hemisphere study are located in areas characterized by MCA dry anomalies. The wet trends of Tunisia and the western Sahel are not represented in the analysis. Ljungqvist et al. (2016) highlight important discrepancies between climate reconstructions and simulations and suggest that much work remains before we can model hydroclimate variability accurately. Furthermore, the authors stress the importance of using palaeoclimate data to place recent and predicted hydroclimate changes in a millennium-long context, a conclusion that we fully endorse based on the findings of our African MCA hydroclimate study.

5.7. Solar forcing?

The MCA forms part of millennial-scale cyclicity that has been documented in a large number of studies in Africa and worldwide (Lüning and Vahrenholz, 2016) which however is still insufficiently understood. Various authors have proposed solar activity changes an important driver for millennial-scale climate variability in Africa (e.g. Chase et al., 2009; Heine and Völk, 2011; Hennekam et al., 2014; Maley and Vernet, 2015; Stager et al., 2003). The subject requires additional integration work to better understand temporal and spatial relationships in more detail. The MCA lies in the second half of a high solar-activity phase that spans 700–1250 CE that is only briefly interrupted by the solar quiet phase of the Oort Minimum (1010–1050 CE) (Fig. 5). Evidence exists that many of the oceanic cycles are influenced by solar forcing, although in a complex way (e.g. Andrews et al., 2015; Georgieva et al., 2012; Heine and Völk, 2011; Sfica et al., 2015; Zhou et al., 2014).

6. Regional data gaps and locations for future research

6.1. Data gaps

Despite a great number of studies in the past 15 years and significant progress, there are still major regional data gaps in our understanding of African MCA hydroclimate. The current lack of suitable reconstructions in those poorly documented areas appears to be mostly due to logistical and security challenges. A key region that requires intensified research is the Sahara where a large area of 5000 × 2000 km is represented by only a handful of reconstructions (Fig. 4). Focused additional studies are also needed for West Africa, in particular the zone along the Atlantic coast and its hinterland from southern Senegal to

Nigeria. Likewise the central part of Africa requires special attention where only few data points are available in an area comprising of the Central African Republic, the Congos, Angola, Zambia, southern Chad and South Sudan. Finally, central and southern Madagascar also need further study.

6.2. Locations and proxies for future research

New high resolution palaeoclimate studies are needed in order to fill the identified data gaps. Additional offshore sediment cores are required along the Atlantic coast from The Gambia to Angola, along the coast of the Indian Ocean from northern Mozambique to Somalia and along the North African Mediterranean coast from the Nile Delta to Morocco. Sebkhas and lagoons offer study opportunities in the coastal transition zones in the Mediterranean and Red Sea areas. Lakes, swamps and peatlands are established onshore palaeoclimate archives and provide a large number of potential project sites in West Africa, central Africa and Madagascar. A useful directory of African Wetlands for orientation was published by Hughes and Hughes (1992). Saharan lakes offer promising potential, as evidenced by the successful climate reconstructions in Lake Yoa in Chad by Lézine et al. (2011). Age-dating of fluvial deposits is to be considered in West and Central Africa in order to reconstruct fluctuations in river discharge over the past millennia.

Caves with unstudied speleothems are located in northern Algeria, Tunisia, Somalia, Reunion, Zambia, northern Zimbabwe, and southern Madagascar. Dendrochronology is another currently underrepresented field that may provide important additional insight into African palaeoclimate of the past millennium (Gebrekirstos et al., 2014). Rock hyrax middens have proved to be useful hydroclimate archives in southern Africa (e.g. Chase et al., 2013; Chase et al., 2009). Chances for preservation of the middens are best in arid regions with annual rainfall of less than 400 mm/year (Chase et al., 2012). Taking the known regional distribution of rock hyrax into account, suitable study areas in northern Africa may be located in the Sahel zone, the Algerian Ahaggar Mountains and at the Red Sea coast. Only little additional palaeoclimate information for Africa is expected to come from mountain ice caps and historical river gauge records because the only available research objects in Eastern Africa (Kilimanjaro) and Egypt (Nilometer) have already been studied.

7. Conclusions

In this study we have compiled a hydroclimatic trend map for the MCA in Africa based on 99 published study locations which are described in detail in the data supplement of this paper. Key hydroclimatic proxy curves have been visualized and compared in a series of 16 correlation panels. Three areas have been identified in Africa in which rainfall seems to have increased during the MCA, namely Tunisia, western Sahel and the majority of southern Africa. At the same time, a reduction in precipitation occurred in the rest of Africa, comprising of NW & NE Africa, West Africa, Eastern Africa and the Winter Rainfall Zone of South Africa. MCA hydroclimate change in Africa appears to have been associated with characteristic phases of ocean cycles, in a similar way as observed in modern climate. Aridity in Morocco typically coincides with the positive phase of the North Atlantic Oscillation (NAO), whilst increased rainfall in the western Sahel is often coupled to the positive phase of the Atlantic Multidecadal Oscillation (AMO). Reduction in rainfall in the region Gulf of Aden/southern Red Sea to Eastern Africa could be linked to a negative Indian Ocean Dipole (IOD) or a derived long-term equivalent Indian Ocean cycle parameter. The Intertropical Convergence Zone (ITCZ) appears to have been shifted pole-wards during the MCA, for both the January and July positions. The identified temporal and spatial variability in African precipitation forms an important calibration data set for model hindcast tests. A robust understanding of pre-industrial hydroclimate change and possible forcings is needed to be able to distinguish between natural and

anthropogenic contributions in modern African rainfall. MCA hydroclimate mapping revealed major data gaps in the Sahara, South Sudan, Somalia, Central African Republic, Democratic Republic of Congo, Angola, northern Mozambique, Zambia and Zimbabwe. Special efforts are needed to fill these gaps, e.g. through a dedicated structured research program in which new multiproxy datasets are created, based on the learnings from previous African MCA studies.

Acknowledgments

We wish to thank all scientists whose case studies form the basis of this palaeoclimate mapping synthesis. We are grateful for provision of tabulated data and valuable discussions to Nerilie Abram, Simone Alin, Andrea Baker, Andy Baker, George Brook, Stephen Burns, Brian Chase, Dennis Darby, Yael Edelman-Furstenberg, Jemma Finch, Lydia Gerullis, Annette Hahn, Rick Hennekam, Martin Hoerling, Kenji Izumi, Sahbi Jaouadi, Kelly Kirsten, Peter Knippertz, Henning Kuhnert, Anne-Marie Lézine, Jean Maley, Laurent Marquer, Raimund Muscheler, Frank Neumann, François Nguetsop, Elin Norström, Bruce Railsback, James Russell, David Ryves, Nick Scroxton, Jaap Sinnighe Damsté, Jenny Sjöström, Curt Stager, Jennifer Tierney, Ilya Usoskin, Stephan Woodborne and many others. A large amount of data was sourced through the PANGAEA online data base and the NOAA National Centers for Environmental Information (NCEI, formerly NCDC), invaluable services which are greatly acknowledged. We are indebted to Jurgis Klaudius and Lloyd's Register for providing the database and correlation software IC™ for this project. The technical IC™ team provided crucial support in initiating the data base and charts: A big thank you to Gemma Crawford, Ashely-Anne Stephen, Linda Stromberg, Oscar Rodriguez, Mario Suarez Maranon and Josep Hernandez for their help. This review forms part of the Medieval Climate Anomaly Mapping Project which has been kindly supported by crowdfunding. We are particularly grateful to Jens Kröger for helping to jump-start the project. Note that this study is fully unrelated to the first author's employment in the hydrocarbon sector and was neither commissioned nor funded by the energy industry. SL undertook this study outside office hours as a private person, trained geoscientist, and former full-time academic. The project was greatly facilitated by Google My Maps which allows to effectively capture and share MCA map data with the climate science community. The vectorised Africa base map in this paper was sourced from <http://www.d-maps.com>, a useful service for which we are thankful. We are grateful to Jean Maley and an anonymous reviewer who greatly helped to improve this manuscript.

Appendix A. Supplementary data

Supplementary data to this article can be found online at <https://doi.org/10.1016/j.palaeo.2018.01.025>.

References

- Alin, S.R., Cohen, A.S., 2003. Lake-level history of Lake Tanganyika, East Africa, for the past 2500 years based on ostracode-inferred water-depth reconstruction. *Palaeogeogr. Palaeoclimatol. Palaeoecol.* 199, 31–49.
- Andrews, M.B., Knight, J.R., Gray, L.J., 2015. A simulated lagged response of the North Atlantic oscillation to the solar cycle over the period 1960–2009. *Environ. Res. Lett.* 10, 054022.
- Armitage, S.J., Bristow, C.S., Drake, N.A., 2015. West African monsoon dynamics inferred from abrupt fluctuations of Lake mega-Chad. *Proc. Natl. Acad. Sci.* 112, 8543–8548.
- Ausseil-Badie, J., Barusseau, J.P., Descamps, C., Salif Diop, E.H., Giresse, P., Pazdur, M., 1991. Holocene deltaic sequence in the Saloum estuary, Senegal. *Quat. Res.* 36, 178–194.
- Badou, D.F., Kapangaziwiri, E., Diekkrüger, B., Houenkpe, J., Afouda, A., 2017. Evaluation of recent hydro-climatic changes in four tributaries of the Niger River basin (West Africa). *Hydroclim. Sci.* 62, 715–728.
- Baioumy, H.M., Kayanne, H., Tada, R., 2010. Reconstruction of lake-level and climate changes in lake Qarun, Egypt, during the last 7000 years. *J. Great Lakes Res.* 36, 318–327.
- Baker, A., Hellstrom, C., Kelly, B.F.J., Mariethoz, G., Trouet, V., 2015. A composite annual-resolution stalagmite record of North Atlantic climate over the last three millennia. *Sci. Rep.* 5. <http://dx.doi.org/10.1038/srep10307>.
- Baker, A., Routh, J., Blaauw, M., Roychoudhury, A.N., 2014. Geochemical records of palaeoenvironmental controls on peat forming processes in the Mfabinet peatland, KwaZulu Natal, South Africa since the late Pleistocene. *Palaeogeogr. Palaeoclimatol. Palaeoecol.* 395, 95–106.
- Barker, P.A., Street-Perrott, F.A., Leng, M.J., Greenwood, P.B., Swain, D.L., Perrott, R.A., Telford, R.J., Ficken, K.J., 2001. A 14,000-year oxygen isotope record from diatom silica in two Alpine Lakes on Mt. Kenya. *Science* 292, 2307–2310.
- Barker, P., Telford, R., Merdaci, O., Williamson, D., Taieb, M., Vincens, A., Gibert, E., 2000. The sensitivity of a Tanzanian crater lake to catastrophic tephra input and four millennia of climate change. *The Holocene* 10, 303–310.
- Breman, E., Gillson, L., Willis, K., 2012. How fire and climate shaped grass-dominated vegetation and forest mosaics in northern South Africa during past millennia. *The Holocene* 22, 1427–1439.
- Brncic, T.M., Willis, K.J., Harris, D.J., Telfer, M.W., Bailey, R.M., 2009. Fire and climate change impacts on lowland forest composition in northern Congo during the last 2580 years from palaeoecological analyses of a seasonally flooded swamp. *The Holocene* 19, 79–89.
- Brncic, T.M., Willis, K.J., Harris, D.J., Washington, R., 2007. Culture or climate? The relative influences of past processes on the composition of the lowland Congo rainforest. *Philos. Trans. R. Soc. B* 362, 229–242.
- Brook, G.A., Marais, E., Srivastava, P., Jordan, T., 2007. Timing of lake-level changes in Etosha Pan, Namibia, since the middle Holocene from OSL ages of relict shorelines in the Okonkwe region. *Quat. Int.* 175, 29–40.
- Brook, G.A., Railsback, L.B., Scott, L., Voarintsoa, N.R.G., Liang, F., 2015. Late Holocene stalagmite and tufa climate records for Wonderwerk Cave: relationships between archaeology and climate in southern Africa. *Afr. Archaeol. Rev.* 32, 669–700.
- Buckles, L.K., Verschuren, D., Weijers, J.W.H., Cocquyt, C., Blaauw, M., Sinnighe Damsté, J.S., 2016. Interannual and (multi-)decadal variability in the sedimentary BIT index of Lake Challa, East Africa, over the past 2200 years: assessment of the precipitation proxy. *Clim. Past* 12, 1243–1262.
- Burns, S.J., Godfrey, L.R., Faina, P., McGee, D., Hardt, B., Ranivoarimanana, L., Randrianasy, J., 2016. Rapid human-induced landscape transformation in Madagascar at the end of the first millennium of the common era. *Quat. Sci. Rev.* 134, 92–99.
- Burrough, S.L., Willis, K.J., 2015. Ecosystem resilience to late-Holocene climate change in the upper Zambezi Valley. *The Holocene* 25, 1811–1828.
- Byrne, M.P., Schneider, T., 2016. Energetic constraints on the width of the intertropical convergence zone. *J. Clim.* 29, 4709–4721.
- Calò, C., Henne, P.D., Eugster, P., Leeuw, J., Gilli, A., Hamann, Y., Mantia, T.L., Pasta, S., Vescovi, E., Tinner, W., 2013. 1200 years of decadal-scale variability of Mediterranean vegetation and climate at Pantelleria Island, Italy. *The Holocene* 23, 1477–1486.
- Chase, B.M., Boom, A., Carr, A.S., Meadows, M.E., Reimer, P.J., 2013. Holocene climate change in southernmost South Africa: rock hyrax middens record shifts in the southern westerlies. *Quat. Sci. Rev.* 82, 199–205.
- Chase, B.M., Lim, S., Chevalier, M., Boom, A., Carr, A.S., Meadows, M.E., Reimer, P.J., 2015. Influence of tropical easterlies in southern Africa's winter rainfall zone during the Holocene. *Quat. Sci. Rev.* 107, 138–148.
- Chase, B.M., Meadows, M.E., Scott, L., Thomas, D.S.G., Marais, E., Sealy, J., Reimer, P.J., 2009. A record of rapid Holocene climate change preserved in hyrax middens from southwestern Africa. *Geology* 37, 703–706.
- Chase, B.M., Scott, L., Meadows, M.E., Gil-Romera, G., Boom, A., Carr, A.S., Reimer, P.J., Truc, L., Valsecchi, V., Quick, L.J., 2012. Rock hyrax middens: a palaeoenvironmental archive for southern African drylands. *Quat. Sci. Rev.* 56, 107–125.
- Chauhan, O.S., Vogelsang, E., Basavaiah, N., Kader, U.S.A., 2010. Reconstruction of the variability of the southwest monsoon during the past 3 ka, from the continental margin of the southeastern Arabian Sea. *J. Quat. Sci.* 25, 798–807.
- Cheddadi, R., Lamb, H.F., Guiot, J., van der Kaars, S., 1998. Holocene climatic change in Morocco: a quantitative reconstruction from pollen data. *Clim. Dyn.* 14, 883–890.
- Cockerton, H.E., Holmes, J.A., Street-Perrott, F.A., Ficken, K.J., 2014. Holocene dust records from the west African Sahel and their implications for changes in climate and land surface conditions. *J. Geophys. Res. Atmos.* 119, 8684–8694.
- Cohen, A.L., Tyson, P.D., 1995. Sea-surface temperature fluctuations during the Holocene off the south coast of Africa: implications for terrestrial climate and rainfall. *The Holocene* 5, 304–312.
- Cremaschi, M., Pelfini, M., Santilli, M., 2006. *Cupressus dupreziana*: a dendroclimatic record for the middle-late Holocene in the central Sahara. *The Holocene* 16, 293–303.
- Crowley, T.J., Lowery, T.S., 2000. How warm was the medieval warm period? *AMBOJ Hum. Environ.* 29, 51–54.
- Curry, B., Henne, P.D., Mesquita-Joanes, F., Marrone, F., Pieri, V., La Mantia, T., Calò, C., Tinner, W., 2016. Holocene paleoclimate inferred from salinity histories of adjacent lakes in southwestern Sicily (Italy). *Quat. Sci. Rev.* 150, 67–83.
- Damnatni, B., Etebaai, I., Benjlani, H., El Khoudri, K., Reddad, H., Taieb, M., 2016. Sedimentology and geochemistry of lacustrine terraces of three Middle Atlas lakes: Paleohydrological changes for the last 2300 cal BP in Morocco (western Mediterranean region). *Quat. Int.* 404, Part B, 163–173.
- Darby, D.A., Ortiz, J.D., Grosch, C.E., Lund, S.P., 2012. 1,500-year cycle in the Arctic oscillation identified in Holocene Arctic sea-ice drift. *Nat. Geosci.* 5, 897–900.
- de Boer, E.J., de Louw, P.G.B., Florens, F.B.V., Baider, C., Hooghiemstra, H., 2014. Climate variability in the SW Indian Ocean from an 8000+ year long multi-proxy record in the Mauritian lowlands shows a middle to late Holocene shift from negative IOD-state to ENSO-state. *Quat. Sci. Rev.* 86, 175–189.
- De Cort, G., Bessem, I., Keppens, E., Mees, F., Cumming, B., Verschuren, D., 2013. Late-Holocene and recent hydroclimatic variability in the central Kenya Rift Valley: the

- sediment record of hypersaline lakes Bogoria, Nakuru and Elementaita. *Palaeogeogr. Palaeoclimatol. Palaeoecol.* 388, 69–80.
- Delworth, T.L., Zhang, R., Mann, M.E., 2007. Decadal to centennial variability of the Atlantic from observations and models. In: Schmittner, A., Chiang, J.C.H., Hemming, S.R. (Eds.), Ocean Circulation: Mechanisms and Impacts—Past and Future Changes of Meridional Overturning. Geophysical Monograph Series 173. American Geophysical Union, pp. 131–148.
- Dong, B., Sutton, R., 2015. Dominant role of greenhouse-gas forcing in the recovery of Sahel rainfall. *Nat. Clim. Chang.* 5, 757–760.
- Dramis, F., Umer, M., Calderoni, G., Haile, M., 2003. Holocene climate phases from buried soils in Tigray (northern Ethiopia): comparison with lake level fluctuations in the main Ethiopian rift. *Quat. Res.* 60, 274–283.
- Edelman-Furstenberg, Y., Almogi-Labin, A., Hemleben, C., 2009. Palaeceanographic evolution of the central Red Sea during the late Holocene. *The Holocene* 19, 117–127.
- Ekbom, A., Stabell, B., 2008. Paleohydrology of Lake Nhuacuti (southern Mozambique), ~400 AD to present. *J. Paleolimnol.* 40, 1127–1141.
- Esper, J., Frank, D., 2009. The IPCC on a heterogeneous medieval warm period. *Clim. Chang.* 94, 267–273.
- Esper, J., Frank, D., Büntgen, U., Verstege, A., Luterbacher, J., Xoplaki, E., 2007. Long-term drought severity variations in Morocco. *Geophys. Res. Lett.* 34.
- Fall, M., Gaye, J.P., Trimborn, P., 2010. Isotope refinement of late Holocene climatic oscillations in the northern coast of Senegal. *Glob. Planet. Chang.* 72, 331–333.
- Finch, J., Marchant, R., Mustaphi, C.J.C., 2016. Ecosystem Change in the South Pare Mountain Bloc, Eastern Arc Mountains of Tanzania. *The Holocene Early Online*. pp. 1–15.
- Fitchett, J.M., Mackay, A.W., Grab, S.W., Bamford, M.K., 2017. Holocene climatic variability indicated by a multi-proxy record from southern Africa's highest wetland. *The Holocene* 27, 638–650.
- Flaux, C., El-Assal, M., Marriner, N., Morhange, C., Rouchy, J.-M., Soulié-Märche, I., Torab, M., 2012. Environmental changes in the Maryut lagoon (northwestern Nile delta) during the last ~2000 years. *J. Archaeol. Sci.* 39, 3493–3504.
- Foerster, V., Vogelsang, R., Junginger, A., Asrat, A., Lamb, H.F., Schaebitz, F., Trauth, M.H., 2015. Environmental change and human occupation of southern Ethiopia and northern Kenya during the last 20,000 years. *Quat. Sci. Rev.* 129, 333–340.
- Fröhlich, L., Knippertz, P., 2008. Identification and global climatology of upper-level troughs at low latitudes. *Meteorol. Z.* 17, 565–573.
- Fröhlich, L., Knippertz, P., Fink, A.H., Hohberger, E., 2013. An objective climatology of tropical plumes. *J. Clim.* 26, 5044–5060.
- Gebrekirstos, A., Bräuning, A., Sassi-Klassen, U., Mbow, C., 2014. Opportunities and applications of dendrochronology in Africa. *Curr. Opin. Environ. Sustain.* 6, 48–53.
- Georgieva, K., Kirov, B., Koucká Knížová, P., Mošna, Z., Kouba, D., Asenovská, Y., 2012. Solar influences on atmospheric circulation. *J. Atmos. Sol. Terr. Phys.* 90–91, 15–25.
- Ghinassi, M., D'Oriano, F., Benvenuti, M., Awramik, S., Bartolini, C., Fedi, M., Ferrari, G., Papini, M., Sagri, M., Talbot, M., 2012. Shoreline fluctuations of Lake Hayk (northern Ethiopia) during the last 3500 years: geomorphological, sedimentary, and isotope records. *Palaeogeogr. Palaeoclimatol. Palaeoecol.* 365–366, 209–226.
- Gitau, W., Camberlin, P., Ogallo, L., Bosire, E., 2017. Trends of intraseasonal descriptors of wet and dry spells over equatorial eastern Africa. *Int. J. Climatol.* <http://dx.doi.org/10.1002/joc.5234>.
- Givati, A., Rosenfeld, D., 2013. The Arctic oscillation, climate change and the effects on precipitation in Israel. *Atmos. Res.* 132, 114–124.
- Granger, R., Meadows, M.E., Hahn, A., Zabel, M., Stut, J.-B.W., Herrmann, N., Schefuß, E., 2017. Late-Holocene dynamics of sea-surface temperature and terrestrial hydrology in southwestern Africa. *The Holocene*. <http://dx.doi.org/10.1177/0959683617744259>.
- Hahn, A., Compton, J.S., Meyer-Jacob, C., Kirsten, K.L., Lucassen, F., Pérez Mayo, M., Schefuß, E., Zabel, M., 2016. Holocene paleo-climatic record from the south African Namaqualand mudbelt: a source to sink approach. *Quat. Int.* 404, Part B, 121–135.
- Hahn, A., Schefuß, E., Andó, S., Cawthra, H.C., Frenzel, P., Kugel, M., Meschner, S., Mollenhauer, G., Zabel, M., 2017. Southern hemisphere anticyclonic circulation drives oceanic and climatic conditions in late Holocene southernmost Africa. *Clim. Past* 13, 649–665.
- Hassan, F.A., 2007. Extreme Nile floods and famines in medieval Egypt (AD 930–1500) and their climatic implications. *Quat. Int.* 173–174, 101–112.
- Hassan, F.A., Hamdan, M.A., Flower, R.J., Keatings, K., 2012. The oxygen and carbon isotopic records in Holocene freshwater mollusc shells from the faiyum paleolakes, Egypt: their palaeoenvironmental and paleoclimatic implications. *Quat. Int.* 266, 175–187.
- Haynes, C.V., Mehringer, P.J., El Sayed Abbas, Z., 1979. Pluvial Lakes of north-western Sudan. *Geogr. J.* 145, 437–445.
- Heine, K., Völkel, J., 2011. Extreme floods around AD 1700 in the northern Namib Desert, Namibia, and in the Orange River catchment, South Africa - were they forced by a decrease of solar irradiance during the little ice age? *Geogr. Pol.* 84, 61–80.
- Hennekam, R., Jilbert, T., Schnetger, B., de Lange, G.J., 2014. Solar forcing of Nile discharge and sapropel S1 formation in the early to middle Holocene eastern Mediterranean. *Paleoceanography* 29, 343–356.
- Hoerling, M., Eischeid, J., Perlitz, J., Quan, X., Zhang, T., Pegion, P., 2012. On the increased frequency of Mediterranean drought. *J. Clim.* 25, 2146–2161.
- Holmgren, K., Öberg, H., 2006. Climate change in southern and eastern Africa during the past millennium and its implications for societal development. *Environ. Dev. Sustain.* 8, 185–195.
- Hua, W., Zhou, L., Chen, H., Nicholson, S.E., Raghavendra, A., Jiang, Y., 2016. Possible causes of the central equatorial African long-term drought. *Environ. Res. Lett.* 11, 124002.
- Huffman, T.N., 1996. Archaeological evidence for climatic change during the last 2000 years in southern Africa. *Quat. Int.* 33, 55–60.
- Huffman, T.N., Woodborne, S., 2016. Archaeology, baobabs and drought: cultural proxies and environmental data from the Mapungubwe landscape, southern Africa. *The Holocene* 26, 464–470.
- Hughes, R.H., Hughes, J.S., 1992. A Directory of African Wetlands. IUCN, UNEP, WCMC.
- Hunt, C.O., Brooks, I., Meneely, J., Brown, D., Buzaian, A., Barker, G., 2011. The Cyrenaican prehistory project 2011: late-Holocene environments and human activity from a cave fill in Cyrenaica, Libya. *Libyan Stud.* 42, 77–87.
- Izumi, K., Lézine, A.M., 2016. Pollen-based biome reconstructions over the past 18,000 years and atmospheric CO₂ impacts on vegetation in equatorial mountains of Africa. *Quat. Sci. Rev.* 152, 93–103.
- Jaouadi, S., Lebreton, V., Bout-Roumazeilles, V., Siani, G., Lakhdar, R., Boussoffara, R., Dezileau, L., Kallel, N., Mannai-Tayech, B., Combourieu-Nebout, N., 2016. Environmental changes, climate and anthropogenic impact in south-east Tunisia during the last 8 kyr. *Clim. Past* 12, 1339–1359.
- Johnson, T.C., Brown, E.T., McManus, J., 2004. Diatom productivity in Northern Lake Malawi during the past 25,000 years: implications for the position of the intertropical convergence zone at millennial and shorter time scales. In: Battarbee, R., Gasse, F., Stickley, C. (Eds.), *Past Climate Variability Through Europe and Africa*. Springer, Netherlands, pp. 93–116.
- Kirsten, K.L., Meadows, M.E., 2016. Late-Holocene palaeolimnological and climate dynamics at Princessvlei, South Africa: evidence from diatoms. *The Holocene* 26, 1371–1381.
- Knippertz, P., Fink, A.H., 2008. Dry-season precipitation in tropical West Africa and its relation to forcing from the extratropics. *Mon. Weather Rev.* 136, 3579–3596.
- Knippertz, P., Fink, A.H., 2009. Prediction of dry-season precipitation in tropical West Africa and its relation to forcing from the extratropics. *Weather Forecast.* 24, 1064–1084.
- Knippertz, P., Martin, J.E., 2005. Tropical plumes and extreme precipitation in subtropical and tropical West Africa. *Q. J. R. Meteorol. Soc.* 131, 2337–2365.
- Kondrashov, D., Feliks, Y., Ghil, M., 2005. Oscillatory modes of extended Nile river records (A.D. 622–1922). *Geophys. Res. Lett.* 32.
- Konecky, B., Russell, J., Huang, Y., Vuille, M., Cohen, L., Street-Perrott, F.A., 2014. Impact of monsoons, temperature, and CO₂ on the rainfall and ecosystems of Mt. Kenya during the common era. *Palaeogeogr. Palaeoclimatol. Palaeoecol.* 396, 17–25.
- Köppen, W., 1918. Klassification der Klimate nach Temperatur, Niederschlag und Jahreslauf. Petermanns Geographische Mitteilungen. (64. pp).
- Kuhnert, H., Mulitz, S., 2011. Multidecadal variability and late medieval cooling of near-coastal sea surface temperatures in the eastern tropical North Atlantic. *Paleoceanography* 26, PA4224.
- Lamb, H.H., 1965. The early medieval warm epoch and its sequel. *Palaeogeogr. Palaeoclim. Palaeoecol.* 1, 13–37.
- Lamb, H., Darbyshire, I., Verschuren, D., 2003. Vegetation response to rainfall variation and human impact in central Kenya during the past 1100 years. *The Holocene* 13, 285–292.
- Lamb, H.F., Leng, M.J., Telford, R.J., Ayenew, T., Umer, M., 2007. Oxygen and carbon isotope composition of authigenic carbonate from an Ethiopian lake: a climate record of the last 2000 years. *The Holocene* 17, 517–526.
- Lamb, P.J., Pepler, R.A., 1987. North Atlantic oscillation: concept and an application. *Bull. Am. Meteorol. Soc.* 68, 1218–1225.
- Lamb, H., Roberts, N., Leng, M., Barker, P., Benkaddour, A., van der Kaars, S., 1999. Lake evolution in a semi-arid montane environment: response to catchment change and hydroclimatic variation. *J. Paleolimnol.* 21, 325–343.
- Lebamba, J., Vincens, A., Maley, J., 2012. Pollen, vegetation change and climate at Lake Barombi Mbo (Cameroon) during the last ca. 33 000 cal yr BP: a numerical approach. *Clim. Past* 8, 59–78.
- Lespez, L., Le Drezent, Y., Garnier, A., Rasse, M., Eichhorn, B., Ozainne, S., Ballouche, A., Neumann, K., Huyscom, E., 2011. High-resolution fluvial records of Holocene environmental changes in the Sahel: the Yamé River at Ounjougou (Mali, West Africa). *Quat. Sci. Rev.* 30, 737–756.
- Lézine, A.M., Zheng, W., Braconnot, P., Krinner, G., 2011. Late Holocene plant and climate evolution at Lake Yoa, northern Chad: pollen data and climate simulations. *Clim. Past* 7, 1351–1362.
- Ljungqvist, F.C., Krusic, P.J., Sundqvist, H.S., Zorita, E., Brattström, G., Frank, D., 2016. Northern hemisphere hydroclimate variability over the past twelve centuries. *Nature* 532, 94–98.
- Losada, T., Rodriguez-Fonseca, B., Mohino, E., Bader, J., Janicot, S., Mechoso, C.R., 2012. Tropical SST and Sahel rainfall: a non-stationary relationship. *Geophys. Res. Lett.* 39.
- Lüning, S., Gaika, M., Vahrenholz, F., 2017. Warming and cooling: the medieval climate anomaly in Africa and Arabia. *Paleoceanography* 32, 1219–1235.
- Lüning, S., Vahrenholz, F., 2016. Chapter 16 - The Sun's Role in Climate A2 - Easterbrook, Don J. *Evidence-based Climate Science*, second edition. Elsevier, pp. 283–305.
- MacKellar, N., New, M., Jack, C., 2014. Observed and modelled trends in rainfall and temperature for South Africa: 1960–2010. *S. Afr. J. Sci.* 110, 13.
- Macklin, M.G., Toonen, W.H.J., Woodward, J.C., Williams, M.A.J., Flaux, C., Marriner, N., Nicoll, K., Verstraeten, G., Spencer, N., Welsby, D., 2015. A new model of river dynamics, hydroclimatic change and human settlement in the Nile Valley derived from meta-analysis of the Holocene fluvial archive. *Quat. Sci. Rev.* 130, 109–123.
- Maley, J., 2010. Climate and palaeoenvironment evolution in north tropical Africa from the end of the tertiary to the upper Quaternary. *Palaeoecology of Africa* vol. 30, an international yearbook of landscape evolution and palaeoenvironments. In: Runge, J. (Ed.), *African Palaeoenvironments and Geomorphic Landscape Evolution*. CRC Press, pp. 227–278.

- Maley, J., Brenac, P., 1998. Vegetation dynamics, palaeoenvironments and climatic changes in the forests of western Cameroon during the last 28,000 years. *B.P. Rev. Palaeobot. Palynol.* 99, 157–187.
- Maley, J., Vernet, R., 2013. Peuples et évolution climatique en Afrique nord-tropicale, de la fin du Néolithique à l'aube de l'époque moderne. *Afriques* 4, 50. <http://dx.doi.org/10.4000/africaires.1209>.
- Maley, J., Vernet, R., 2015. Populations and climatic evolution in north tropical Africa from the end of the Neolithic to the dawn of the modern era. *Afr. Archaeol. Rev.* 32, 179–232.
- Mann, M.E., Zhang, Z., Rutherford, S., Bradley, R.S., Hughes, M.K., Shindell, D., Ammann, C., Faluvegi, G., Ni, F., 2009. Global signatures and dynamical origins of the little ice age and medieval climate anomaly. *Science* 326, 1256–1260.
- Marquer, L., Pomer, S., Abichou, A., Schulz, E., Kaniewski, D., Van Campo, E., 2008. Late Holocene high resolution palaeoclimatic reconstruction inferred from Sebkha Mhabeul, southeast Tunisia. *Quat. Res.* 70, 240–250.
- Martin, E.R., Thorncroft, C.D., 2014. The impact of the AMO on the west African monsoon annual cycle. *Q. J. R. Meteorol. Soc.* 140, 31–46.
- Masih, I., Maskey, S., Mussá, F.E.F., Trambauer, P., 2014. A review of droughts on the African continent: a geospatial and long-term perspective. *Hydrol. Earth Syst. Sci.* 18, 3635–3649.
- Matsumoto, K., Burney, D.A., 1994. Late Holocene environments at Lake Mitsinjo, northwestern Madagascar. *The Holocene* 4, 16–24.
- McGregor, H.V., Dupont, L., Stut, J.-B.W., Kuhlmann, H., 2009. Vegetation change, goats, and religion: a 2000-year history of land use in southern Morocco. *Quat. Sci. Rev.* 28, 1434–1448.
- Mills, K., Ryves, D.B., Anderson, N.J., Bryant, C.L., Tyler, J.J., 2014. Expressions of climate perturbations in western Ugandan crater lake sediment records during the last 1000 years. *Clim. Past* 10, 1581–1601.
- Mulitz, S., Heslop, D., Pittaurová, D., Fischer, H.W., Meyer, I., Stut, J.-B., Zabel, M., Mollenhauer, G., Collins, J.A., Kuhnhert, H., Schulz, M., 2010. Increase in African dust flux at the onset of commercial agriculture in the Sahel region. *Nature* 466, 226–228.
- Mustapha, Y., Mohamed, B., 2015. A 1000-year record from El-Ghorra mountain (NE Algeria): Mediterranean vegetation dynamic in response to climatic variation. In: *Ecology, Environment and Conservation Paper*, vol. 21. pp. 1189–1198.
- Nash, D.J., De Cort, G., Chase, B.M., Verschuren, D., Nicholson, S.E., Shanahan, T.M., Asrat, A., Lézine, A.-M., Grab, S.W., 2016. African hydroclimatic variability during the last 2000 years. *Quat. Sci. Rev.* 154, 1–22.
- Nash, D.J., Meadows, M.E., Gulliver, V.L., 2006. Holocene environmental change in the Okavango panhandle, northwest Botswana. *Quat. Sci. Rev.* 25, 1302–1322.
- Neumann, F.H., Botha, G.A., Scott, L., 2014. 18,000 years of grassland evolution in the summer rainfall region of South Africa: evidence from Mahwaqa Mountain, KwaZulu-Natal. *Veg. Hist. Archaeobotany* 23, 665–681.
- Neumann, F.H., Scott, L., Bousman, C.B., van As, L., 2010. A Holocene sequence of vegetation change at Lake Eteza, coastal KwaZulu-Natal, South Africa. *Rev. Palaeobot. Palynol.* 162, 39–53.
- Neumann, F.H., Stager, J.C., Scott, L., Venter, H.J.T., Weyhenmeyer, C., 2008. Holocene vegetation and climate records from Lake Sibaya, KwaZulu-Natal (South Africa). *Rev. Palaeobot. Palynol.* 152, 113–128.
- Ngomanda, A., Chepstow-Lusty, A., Makaya, M., Schevin, P., Maley, J., Fontugne, M., Oslisly, R., Rabenkogo, N., Jolly, D., 2005. Vegetation changes during the past 1300 years in western equatorial Africa: a high-resolution pollen record from Lake Kamalee, lope reserve, Central Gabon. *The Holocene* 15, 1021–1031.
- Ngomanda, A., Jolly, D., Bentaleb, I., Chepstow-Lusty, A., Makaya, M., Maley, J., Fontugne, M., Oslisly, R., Rabenkogo, N., 2007. Lowland rainforest response to hydrological changes during the last 1500 years in Gabon, western equatorial Africa. *Quat. Res.* 67, 411–425.
- Nguetsop, V.F., Servant-Vildary, S., Servant, M., 2004. Late Holocene climatic changes in west Africa, a high resolution diatom record from equatorial Cameroon. *Quat. Sci. Rev.* 23, 591–609.
- Nicholson, S.E., 2000. The nature of rainfall variability over Africa on time scales of decades to millennia. *Glob. Planet. Chang.* 26, 137–158.
- Nicholson, S.E., 2013. The west African Sahel: a review of recent studies on the rainfall regime and its interannual variability. *ISRN Meteorol.* 2013, 32.
- Nicholson, S., 2016. The Turkana low-level jet: mean climatology and association with regional aridity. *Int. J. Climatol.* 36, 2598–2614.
- Nizou, J., Hanebuthe, T.J.J., Heslop, D., Schwenk, T., Palamenghi, L., Stut, J.-B., Henrich, R., 2010. The Senegal River mud belt: a high-resolution archive of paleoclimatic change and coastal evolution. *Mar. Geol.* 278, 150–164.
- Nizou, J., Hanebuthe, T.J.J., Vogt, C., 2011. Deciphering signals of late Holocene fluvial and aeolian supply from a shelf sediment depocentre off Senegal (north-west Africa). *J. Quat. Sci.* 26, 411–421.
- Norström, E., Neumann, F.H., Scott, L., Smittenberg, R.H., Holmstrand, H., Lundqvist, S., Snowball, Sundqvist, H.S., Risberg, J., Bamford, M., 2014. Late Quaternary vegetation dynamics and hydro-climate in the Drakensberg, South Africa. *Quat. Sci. Rev.* 105, 48–65.
- Norström, E., Scott, L., Partridge, T.C., Risberg, J., Holmgren, K., 2009. Reconstruction of environmental and climate changes at Braamhoek wetland, eastern escarpment South Africa, during the last 16,000 years with emphasis on the Pleistocene-Holocene transition. *Palaeogeogr. Palaeoclimatol. Palaeoecol.* 271, 240–258.
- Nouaceur, Z., Murarescu, O., 2016. Rainfall variability and trend analysis of annual rainfall in North Africa. *Int. J. Atmos. Sci.* 2016, 12.
- Öberg, H., Norström, E., Malmström Ryner, M., Holmgren, K., Westerberg, L.-O., Risberg, J., Eddudóttir, S.D., Andersen, T.J., Muzuka, A., 2013. Environmental variability in northern Tanzania from AD 1000 to 1800, as inferred from diatoms and pollen in Lake Duluti. *Palaeogeogr. Palaeoclimatol. Palaeoecol.* 374, 230–241.
- Ondoulami, R.C., Akinsanola, A.A., 2017. Recent assessment of west African summer monsoon daily rainfall trends. *Weather* 1–4.
- Olsen, J., Anderson, N.J., Knudsen, M.F., 2012. Variability of the North Atlantic oscillation over the past 5,200 years. *Nat. Geosci.* 5, 808–812.
- Ongoma, V., Chen, H., 2017. Temporal and spatial variability of temperature and precipitation over East Africa from 1951 to 2010. *Meteorol. Atmos. Phys.* 129, 131–144.
- PAGES 2k Consortium, 2013. Continental-scale temperature variability during the past two millennia. *Nat. Geosci.* 6, 339–346.
- Park, J.-Y., Bader, J., Matei, D., 2016. Anthropogenic Mediterranean warming essential driver for present and future Sahel rainfall. *Nat. Clim. Chang.* 6, 941–945.
- Prasad, S., Anoop, A., Riedel, N., Sarkar, S., Menzel, P., Basavaiah, N., Krishnan, R., Fuller, D., Plessen, B., Gaye, B., Röhl, U., Wilkes, H., Sachse, D., Sawant, R., Wiesner, M.G., Stebich, M., 2014. Prolonged monsoon droughts and links to Indo-Pacific warm pool: a Holocene record from Lonar Lake, central India. *Earth Planet. Sci. Lett.* 391, 171–182.
- Railsback, B.L., Brook, G.A., Webster, J.W., 1999. Petrology and paleoenvironmental significance of detrital sand and silt in a stalagmite from Drottsky's cave, Botswana. *Phys. Geogr.* 20, 331–347.
- Revel, M., Ducassou, E., Skonieczny, C., Colin, C., Bastian, L., Bosch, D., Migeon, S., Mascle, J., 2015. 20,000 years of Nile River dynamics and environmental changes in the Nile catchment area as inferred from Nile upper continental slope sediments. *Quat. Sci. Rev.* 130, 200–221.
- Riedel, F., Erhardt, S., Chauke, C., Kossler, A., Shemang, E., Tarasov, P., 2012. Evidence for a permanent lake in Sua pan (Kalahari, Botswana) during the early centuries of the last millennium indicated by distribution of baobab trees (*Adansonia digitata*) on "Kubu Island". *Quat. Int.* 253, 67–73.
- Rowell, D.P., Booth, B.B., Nicholson, S.E., Good, P., 2015. Reconciling past and future rainfall trends over East Africa. *J. Clim.* 28, 9768–9788.
- Russell, J.M., Johnson, T.C., 2005. A high-resolution geochemical record from Lake Edward, Uganda Congo and the timing and causes of tropical African drought during the late Holocene. *Quat. Sci. Rev.* 24, 1375–1389.
- Russell, J.M., Johnson, T.C., 2007. Little ice age drought in equatorial Africa: intertropical convergence zone migrations and El Niño-southern oscillation variability. *Geology* 35, 21–24.
- Russell, J.M., Verschuren, D., Eggermont, H., 2007. Spatial complexity of 'little ice age' climate in East Africa: sedimentary records from two crater lake basins in western Uganda. *The Holocene* 17, 183–193.
- Ryves, D.B., Mills, K., Bennike, O., Brodersen, K.P., Lamb, A.L., Leng, M.J., Russell, J.M., Ssemmanda, I., 2011. Environmental change over the last millennium recorded in two contrasting crater lakes in western Uganda, eastern Africa (lakes Kasenda and Wandakara). *Quat. Sci. Rev.* 30, 555–569.
- Sachs, J.P., Sachse, D., Smittenberg, R.H., Zhang, Z., Battisti, D.S., Golubic, S., 2009. Southward movement of the Pacific intertropical convergence zone AD 1400–1850. *Nat. Geosci.* 2, 519–525.
- Saji, N.H., Goswami, B.N., Vinayachandran, P.N., Yamagata, T., 1999. A dipole mode in the tropical Indian Ocean. *Nature* 401, 360–363.
- Sandeep, K., Shankar, R., Warrier, A.K., Weijian, Z., Xuefeng, L., 2015. The environmental magnetic record of palaeoenvironmental variations during the past 3100 years: a possible solar influence? *J. Appl. Geophys.* 118, 24–36.
- Schneider, T., Bischoff, T., Haug, G.H., 2014. Migrations and dynamics of the intertropical convergence zone. *Nature* 513, 45–53.
- Scott, L., Bousman, C.B., Nyakale, M., 2005. Holocene pollen from swamp, cave and hyrax dung deposits at Blydefontein (Kikvorsberge), Karoo, South Africa. *Quat. Int.* 129, 49–59.
- Scroxton, N., Burns, S.J., McGee, D., Hardt, B., Godfrey, L.R., Ranivoharimanana, L., Faina, P., 2017. Hemispherically-in-phase precipitation variability over the last 1700 years in a Madagascar speleothem record. *Quat. Sci. Rev.* 164, 25–36.
- Sfica, L., Voiculescu, M., Huth, R., 2015. The influence of solar activity on action centres of atmospheric circulation in North Atlantic. *Ann. Geophys.* 33, 207–215.
- Shanahan, T.M., Overpeck, J.T., Anchukaitis, K.J., Beck, J.W., Cole, J.E., Dettman, D.L., Peck, J.A., Scholz, C.A., King, J.W., 2009. Atlantic forcing of persistent drought in West Africa. *Science* 324, 377–380.
- Shankar, R., Prabhu, C.N., Warrier, A.K., Kumar, G.T.V., Sekar, B., 2006. A multi-decadal rock magnetic record of monsoonal variations during the past 3,700 years from a tropical Indian tank. *J. Geol. Soc. India* 68, 447–459.
- Skinner, C.B., Poulsen, C.J., 2016. The role of fall season tropical plumes in enhancing Saharan rainfall during the African humid period. *Geophys. Res. Lett.* 43, 349–358.
- Sletten, H.R., Railsback, L.B., Liang, F., Brook, G.A., Marais, E., Hardt, B.F., Cheng, H., Edwards, R.L., 2013. A petrographic and geochemical record of climate change over the last 4600 years from a northern Namibia stalagmite, with evidence of abruptly wetter climate at the beginning of southern Africa's iron age. *Palaeogeogr. Palaeoclimatol. Palaeoecol.* 376, 149–162.
- Ssemmanda, I., Ryves, D.B., Bennike, O., Appleby, P.G., 2005. Vegetation history in western Uganda during the last 1200 years: a sediment-based reconstruction from two crater lakes. *The Holocene* 15, 119–132.
- Stager, J.C., Cocquyt, C., Bonneville, R., Weyhenmeyer, C., Bowerman, N., 2009. A late Holocene paleoclimatic history of Lake Tanganyika, East Africa. *Quat. Res.* 72, 47–56.
- Stager, J.C., Cumming, B.F., Meeker, L.D., 2003. A 10,000-year high-resolution diatom record from Pilkington Bay, Lake Victoria, East Africa. *Quat. Res.* 59, 172–181.
- Stager, J.C., Mayewski, P.A., White, J., Chase, B.M., Neumann, F.H., Meadows, M.E., King, C.D., Dixon, D.A., 2012a. Precipitation variability in the winter rainfall zone of South Africa during the last 1400 yr linked to the austral westerlies. *Clim. Past* 8, 877–887.
- Stager, J.C., Mayewski, P.A., White, J., Chase, B.M., Neumann, F.H., Meadows, M.E., King, C.D., Dixon, D.A., 2012b. Verlorenvlei, South Africa 1400-year diatom abundance data, IGBP PAGES/world data center for paleoclimatology, data contribution

- series # 2012-057, NOAA/NCDC paleoclimatology program, Boulder CO, USA. <ftp://ftp.ncdc.noaa.gov/pub/data/paleo/paleolimnology/africa/verlorenvlei2012.txt>.
- Stager, C.J., Ryves, D., Cumming, F.B., Meeker, D.L., Beer, J., 2005. Solar variability and the levels of Lake Victoria, East Africa, during the last millennium. *J. Paleolimnol.* 33, 243–251.
- Stager, J.C., Ryves, D.B., King, C., Madson, J., Hazzard, M., Neumann, F.H., Maud, R., 2013. Late Holocene precipitation variability in the summer rainfall region of South Africa. *Quat. Sci. Rev.* 67, 105–120.
- Steinhilber, F., Abreu, J.A., Beer, J., Brunner, I., Christl, M., Fischer, H., Heikkilä, U., Kubik, P.W., Mann, M., McCracken, K.G., Miller, H., Miyahara, H., Oerter, H., Wilhelms, F., 2012. 9,400 years of cosmic radiation and solar activity from ice cores and tree rings. *Proc. Natl. Acad. Sci.* 109, 5967–5971.
- Stokes, S., Bailey, R.M., Fedoroff, N., O'Maragh, K.E., 2004. Optical dating of Aeolian dynamism on the west African Sahelian margin. *Geomorphology* 59, 281–291.
- Street-Perrott, F.A., Holmes, J.A., Waller, M.P., Allen, M.J., Barber, N.G.H., Fothergill, P.A., Harkness, D.D., Ivanovich, M., Kroon, D., Perrott, R.A., 2000. Drought and dust deposition in the west African Sahel: a 5500-year record from Kajemarum oasis, northeastern Nigeria. *The Holocene* 10, 293–302.
- Taye, M.T., Willems, P., 2012. Temporal variability of hydroclimatic extremes in the Blue Nile basin. *Water Resour. Res.* 48.
- Thamban, M., Kawahata, H., Rao, V., 2007. Indian summer monsoon variability during the holocene as recorded in sediments of the Arabian Sea: timing and implications. *J. Oceanogr.* 63, 1009–1020.
- Thevenon, F., Williamson, D., Vincens, A., Taieb, M., Merdaci, O., Decobert, M., Buchet, G., 2003. A late-Holocene charcoal record from Lake Masoko, SW Tanzania: climatic and anthropologic implications. *The Holocene* 13, 785–792.
- Thompson, L.G., Mosley-Thompson, E., Davis, M.E., Henderson, K.A., Brecher, H.H., Zagorodnov, V.S., Mashirota, T.A., Lin, P.-N., Mikhaleko, V.N., Hardy, D.R., Beer, J., 2002. Kilimanjaro ice Core records: evidence of Holocene climate change in tropical Africa. *Science* 298, 589–593.
- Tierney, J.E., Russell, J.M., Sinnninghe Damsté, J.S., Huang, Y., Verschuren, D., 2011. Late quaternary behavior of the east African monsoon and the importance of the Congo air boundary. *Quat. Sci. Rev.* 30, 798–807.
- Tierney, J.E., Smerdon, J.E., Anchukaitis, K.J., Seager, R., 2013. Multidecadal variability in east African hydroclimate controlled by the Indian Ocean. *Nature* 493, 389–392.
- Tierney, J.E., Ummenhofer, C.C., deMenocal, P.B., 2015. Past and future rainfall in the horn of Africa. *Sci. Adv.* 1.
- Ting, M., Kushnir, Y., Seager, R., Li, C., 2011. Robust features of Atlantic multi-decadal variability and its climate impacts. *Geophys. Res. Lett.* 38, 1–6.
- Trouet, V., Esper, J., Graham, N.E., Baker, A., Scourse, J.D., Frank, D.C., 2009. Persistent positive North Atlantic oscillation mode dominated the medieval climate anomaly. *Science* 324, 78–80.
- Verdon-Kidd, D.C., Kiem, A.S., 2014. Synchronicity of historical dry spells in the southern hemisphere. *Hydrol. Earth Syst. Sci.* 18, 2257–2264.
- Verschuren, D., 2001. Reconstructing fluctuations of a shallow east African lake during the past 1800 yrs from sediment stratigraphy in a submerged crater basin. *J. Paleolimnol.* 25, 297–311.
- Verschuren, D., 2004. Decadal and century-scale climate variability in tropical Africa during the past 2000 years. In: Battarbee, R.W., Gasse, F., Stickley, C.E. (Eds.), *Past Climate Variability through Europe and Africa*. Springer Netherlands, Dordrecht, pp. 139–158.
- Verschuren, D., Laird, K.R., Cumming, B.F., 2000. Rainfall and drought in equatorial east Africa during the past 1,100 years. *Nature* 403, 410–414.
- Vincens, A., Williamson, D., Thevenon, F., Taieb, M., Buchet, G., Decobert, M., Thouveny, N., 2003. Pollen-based vegetation changes in southern Tanzania during the last 4200 years: climate change and/or human impact. *Palaeogeogr. Palaeoclimatol. Palaeoecol.* 198, 321–334.
- Voarintsoa, N.R.G., Railsback, L.B., Brook, G.A., Wang, L., Kathayat, G., Cheng, H., Li, X., Edwards, R.L., Rakotondrazafy, A.F.M., Madison Razanatseheno, M.O., 2017. Three distinct Holocene intervals revealed in NW Madagascar: evidence from two stalagmites from two caves, and implications for ITCZ dynamics. *Clim. Past Discuss.* 2017, 1–37.
- Wassenburg, J.A., Immenhauser, A., Richter, D.K., Niedermayr, A., Riechelmann, S., Fietzke, J., Scholz, D., Jochum, K.P., Fohlmeister, J., Schröder-Ritzrau, A., Sabau, A., Riechelmann, D.F.C., Schneider, L., Esper, J., 2013. Moroccan speleothem and tree ring records suggest a variable positive state of the North Atlantic oscillation during the medieval warm period. *Earth Planet. Sci. Lett.* 375, 291–302.
- Williams, M.A.J., Williams, F.M., Duller, G.A.T., Munro, R.N., El Tom, O.A.M., Barrows, T.T., Macklin, M., Woodward, J., Talbot, M.R., Haberlah, D., Fluin, J., 2010. Late quaternary floods and droughts in the Nile valley, Sudan: new evidence from optically stimulated luminescence and AMS radiocarbon dating. *Quat. Sci. Rev.* 29, 1116–1137.
- Woodborne, S., Gandiwa, P., Hall, G., Patrut, A., Finch, J., 2016. A regional stable carbon isotope dendro-climatology from the south African summer rainfall area. *PLoS One* 11, e0159361.
- Woodborne, S., Hall, G., Robertson, I., Patrut, A., Rouault, M., Loader, N.J., Hofmeyr, M., 2015. A 1000-year carbon isotope rainfall proxy record from South African baobab trees (*Adansonia digitata* L.). *PLoS One* 10, e0124202.
- Wündsch, M., Haberzettl, T., Kirsten, K.L., Kasper, T., Zabel, M., Dietze, E., Baade, J., Daut, G., Meschner, S., Meadows, M.E., Müsibacher, R., 2016. Sea level and climate change at the southern cape coast, South Africa, during the past 4.2 kyr. *Palaeogeogr. Palaeoclimatol. Palaeoecol.* 446, 295–307.
- Zhang, R., Delworth, T.L., 2006. Impact of Atlantic multidecadal oscillations on India/Sahel rainfall and Atlantic hurricanes. *Geophys. Res. Lett.* 33.
- Zhang, Q., Holmgren, K., Sundqvist, H., 2015. Decadal rainfall dipole oscillation over southern Africa modulated by variation of austral summer Land–Sea contrast along the East Coast of Africa. *J. Atmos. Sci.* 72, 1827–1836.
- Zhao, X., Dupont, L., Scheufuß, E., Meadows, M.E., Hahn, A., Wefer, G., 2016. Holocene vegetation and climate variability in the winter and summer rainfall zones of South Africa. *The Holocene* 26 (6), 843–857.
- Zhou, L., Tinsley, B., Huang, J., 2014. Effects on winter circulation of short and long term solar wind changes. *Adv. Space Res.* 54, 2478–2490.
- Zielhofer, C., Faust, D., Linstädter, J., 2008. Late Pleistocene and Holocene alluvial archives in the southwestern Mediterranean: changes in fluvial dynamics and past human response. *Quat. Int.* 181, 39–54.
- Zorzi, C., Sanchez Goñi, M.F., Anupama, K., Prasad, S., Hanquiez, V., Johnson, J., Giosan, L., 2015. Indian monsoon variations during three contrasting climatic periods: the Holocene, Heinrich Stadial 2 and the last interglacial–glacial transition. *Quat. Sci. Rev.* 125, 50–60.